Summer 6-20-2022

EMPLACEMENT OF THE DADEVILLE COMPLEX OF THE SOUTHERNMOST INNER PIEDMONT WITHIN THE 7.5 MIN. CUSSETA QUADRANGLE, CHAMBERS COUNTY, ALABAMA: CHANNEL FLOW, KLIPPE KINEMATICS, OR OROGEN PARALLEL TRANSLATION

Timothy Black

EMPLACEMENT OF THE DADEVILLE COMPLEX OF THE SOUTHERNMOST INNER PIEDMONT WITHIN THE 7.5 MIN. CUSSETA QUADRANGLE, CHAMBERS COUNTY, ALABAMA: CHANNEL FLOW, KLIPPE KINEMATICS, OR OROGEN PARALLEL TRANSLATION

by

Chantz Black

A Thesis
Submitted to the Graduate School,
the College of Arts and Sciences
and the School of Biological, Environmental, and Earth Sciences
at The University of Southern Mississippi
in Partial Fulfillment of the Requirements
for the Degree of Master of Science

Approved by:

Dr. Jeremy Deans, Committee Chair
Dr. Frank Heitmuller
Dr. Mark Puckett

August 2022

Published by the Graduate School

THE UNIVERSITY OF SOUTHERN MISSISSIPPI

ABSTRACT

The Appalachian Mountains have a complex geologic history spanning three orogenic periods, the Taconic, the Acadian/Neoacadian, and Alleghanian orogenies. The Inner Piedmont of the Appalachian Mountains within Alabama contains two distinct lithologic complexes, the Dadeville Complex, and the Opelika Complex separated by the Stonewall Line. These complexes were formed during an arc-back arc fringing system during the Taconic orogeny and emplaced and recorded peak metamorphism during the Acadian orogeny.

The Dadeville Complex is an allochthonous arc terrain built on extended Laurentian crust. The mode of transportation and accretion after formation is not well understood, which has implications for the role of modes of accretion during mountain building events. Three hypotheses of transportation of the Dadeville Complex have been proposed: 1. channel/crustal flow along the margin, 2. klippe thrust movement perpendicular to the margin and, 3. translation along margin-parallel shear zones.

F1 folds with lineations trending N-S were created during peak metamorphism during the Acadian orogeny when shortening was occurring E-W synchronous with emplacement of migmatites within the Dadeville Complex and collision between the IP and DC. F2 folds are upright and trend E-W from N-S shortening, which may have occurred shortly after peak metamorphism, overprinting most F1 structures with lineations trending E. These results suggest that klippe kinematics with a component of orogen parallel translation, with modifications to these models, were the primary mode of translation for the Dadeville Complex. Additionally, the Stonewall Line shows evidence

for being a weakly developed shear zone showing dip-slip motion within the Cusseta quadrangle.

ACKNOWLEDGMENTS

I would like to thank the Department of the Interior, USGS, and the Geological Survey of Alabama for their financial support through the Department of the Interior USGS EDMAP program in coordination with the Geological Survey of Alabama. This project has completely reshaped my understanding of the Appalachian Mountains and Alabama geology, and for that I am grateful.

I would also like to sincerely thank my advisor and long-time instructor Dr. Jeremy Deans for the overwhelming support, guidance, and encouragement through this process. Dr. Deans has been nothing short of an amazing advisor and instructor. His unwavering patience and keen geologic insight while pushing me to be a better person and geologist have been greatly appreciated through these last few years; I could not have done it without him.

DEDICATION

To my wife Marissa, and our daughter Mia. Thank you for fully supporting my geologic endeavors throughout these past few years. With the start of the Covid-19 pandemic in 2020 beginning as soon as my research started, the death of a close family member in 2021, and the birth of our daughter in 2022, these past few years have been nothing short of crazy. Thank you, Marissa, for always being there for me and pushing me to my fullest potential. Mia, you are the light of my life. Your dad loves you very much and the joy you bring me keeps me pushing forward. I love you both so much.

TABLE OF CONTENTS

LIST OF TABLES

LIST OF ILLUSTRATIONS

LIST OF ABBREVIATIONS

AS	Agricola Schist
DCC	Dadeville Complex
FMG	Farmville Metagranite
FZ	Fault Zone
IP	Inner Piedmont
LS	Loachapoka Schist
OCC	Opelika Complex
RCA	Ropes Creek Amphibolite
WG	Waverly Gneiss

CHAPTER I - INTRODUCTION

The Appalachian Mountains formed over three distinct orogenic events, the Taconian (Taconic), Acadian/Neoacadian, and the Alleghanian orogenies. The Taconian orogeny, which took place in the Middle Ordovician to Late Ordovician (~470-445 Ma), is documented as the first major Paleozoic orogenic event in the Appalachian Mountains (Drummond, et al., 1997; Hatcher and Merschat, 2006; Ma, et al., 2019). The Taconian orogeny is responsible for the creation of most of the igneous rocks within the Appalachian Mountains. The Acadian (~404-380 Ma), Neoacadian (~380-340 Ma), and the Alleghanian (~325-260 Ma) events overprinted the Taconic structures through mineral recrystallization and peak metamorphism during the Acadian-Neoacadian orogenies creating certain zonal boundaries, like the Brevard Zone, Stonewall Line, and Towaliga Fault Zone with reactivation occurring during the Alleghanian orogeny (Steltenpohl, 1988; Goldberg and Steltenpohl, 1990; Ma, et al., 2019). The last recorded movement along these fault zones coincides with the Alleghanian orogeny and is dextral and normal (Steltenpohl, 1988; Tull and Holm, 2005; Hatcher and Merschat, 2006).

The Inner Piedmont (IP) is one of the largest sillimanite-bearing terranes in the world, where metamorphic grade remained at or above sillimanite-bearing across most of the IP until it decreases to kyanite and garnet-bearing on the eastern and western flanks (Merschat et al., 2005; Hatcher and Merschat, 2006). The IP consists of medium- to high-grade amphibolite facies of para/ortho-gneisses that extend from North Carolina to the Coastal Plain of Alabama (Merschat et al., 2005). Shallow-dipping foliation and a stack of gently dipping crystalline thrust sheets is how the Inner Piedmont is traditionally characterized.

The Inner Piedmont of Alabama consists of two primary lithologic complexes, the Dadeville Complex and Opelika Complex, sometimes denoted as the Opelika Group, which are constrained by the Brevard Fault Zone to the north, separating the Eastern Blue Ridge from the IP, and the Towaliga Fault Zone, separating the IP from the Pine Mountain Window Proterozoic Eon basement rocks, to the south (Fig. 1.1). The IP has a broad NE plunging syncline, the Tallassee syncline, suggested to be formed by a klippe feature (Farris et al., 2017; Tull et al., 2018). The Stonewall Line is the boundary between the two complexes, but the nature of the boundary is not well constrained, having been reported as either an unconformity or a fault zone (Bentley and Neathery, 1970).

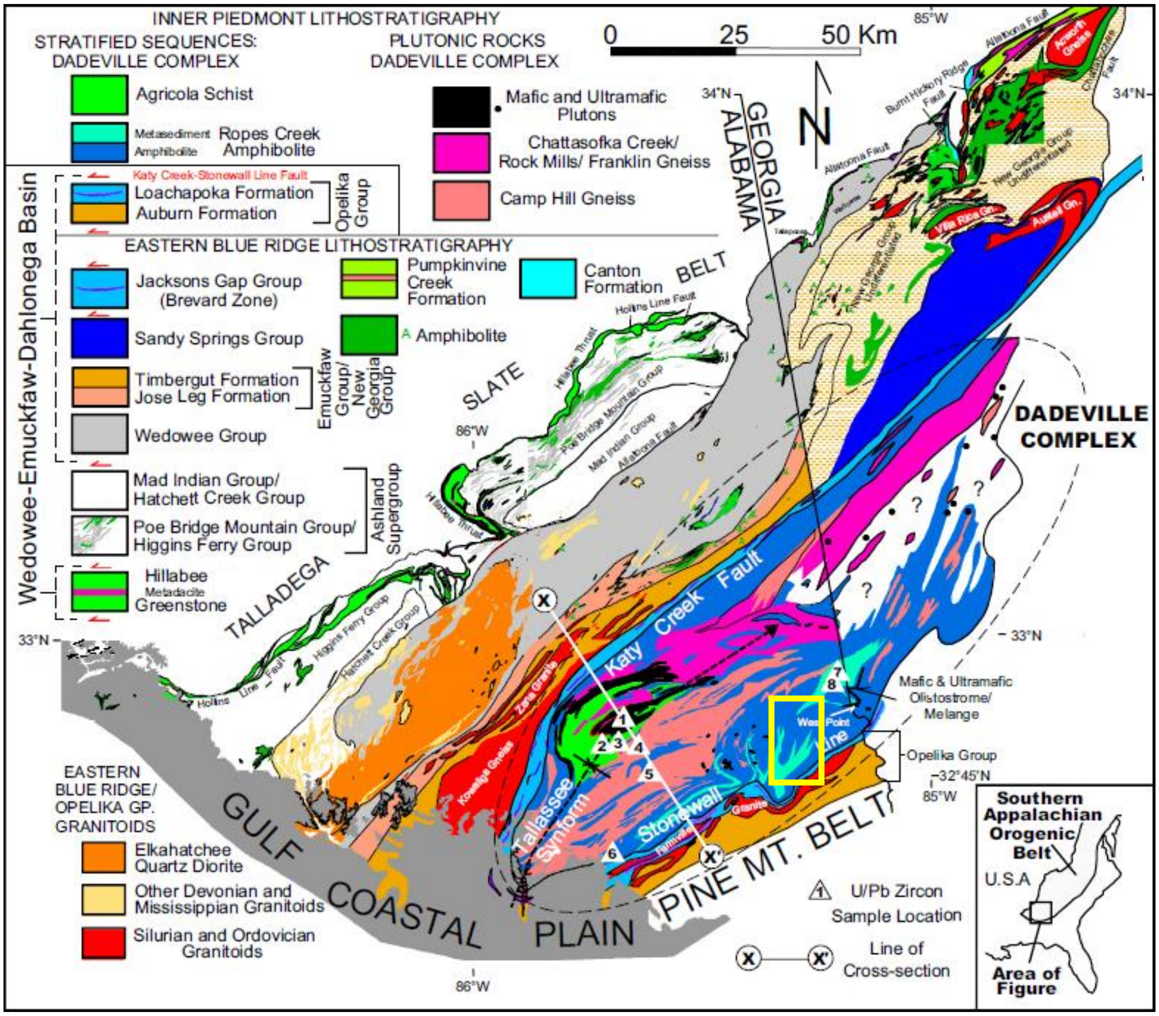

Figure 1.1

Regional geologic map of the southwestern Appalachian orogen showing the components of the Dadeville Complex. Study area outlined in yellow (modified from Farris et al., 2017 & Tull et al., 2018).

Reports by several authors suggest that the Dadeville Complex was moved by means of either translation (Fig. 1.2) (Steltenpohl, 1988; Ma et al., 2019), and/or klippe kinematics (shortening perpendicular to the margin) along the Brevard Fault Zone (Fig. 1.3), Stonewall Line, and to some extent the Towaliga Fault Zones (Sears et al., 1981, Farris et al., 2017; Tull et al., 2018). These hypotheses suggest that all translation was along major shear zones and internal strain within complex was limited. Additionally, Merschat et al. (2005) and Hatcher and Merschat (2006) suggested crustal flow is recorded in the Tugaloo Terrane, Inner Piedmont, in South Carolina and Georgia from the Acadian orogeny (Fig. 1.4). The Tugaloo Terrane is part of the IP and is lithologically similar to the Dadeville Complex. This similarity may indicate that the Dadeville Complex experienced similar internal strain and translation through channel flow as it was pinned against Laurentian basement and the Carolina superterrane during accretion.

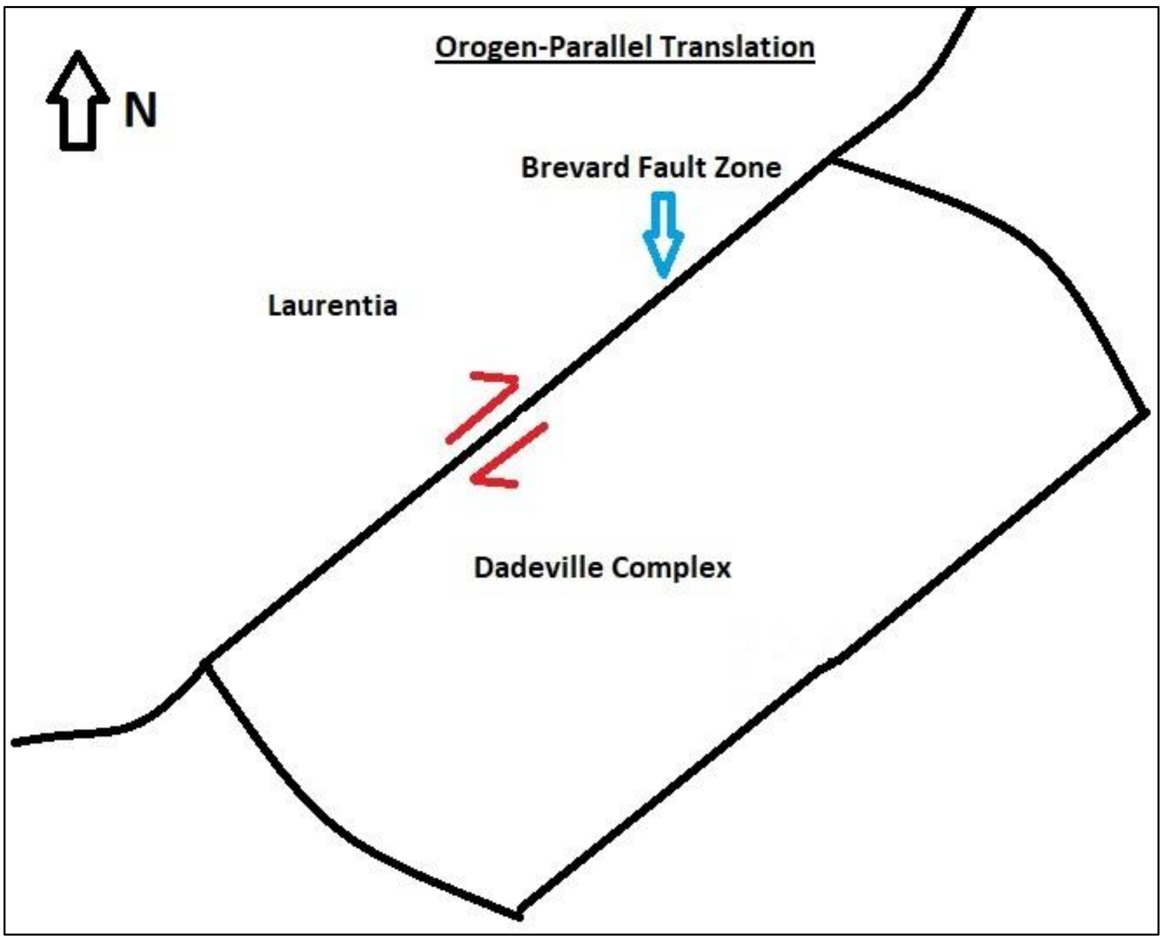

Figure 1.2

Simplified model illustration of orogen-parallel translation.

One goal of this study was to determine if different modes of movement can be identified by looking at zonal boundaries, specifically the Stonewall Line, and the associated kinematics (e.g., dip-slip, strike-slip, etc.), along with internal deformation moving away from the Stonewall Line into the Dadeville Complex and Opelika Complex. This project considered both the regional (mapping) and microscopic level (thin sections), which allowed for the different kinematic models of Dadeville and Opelika Complex formation and evolution to be better constrained.

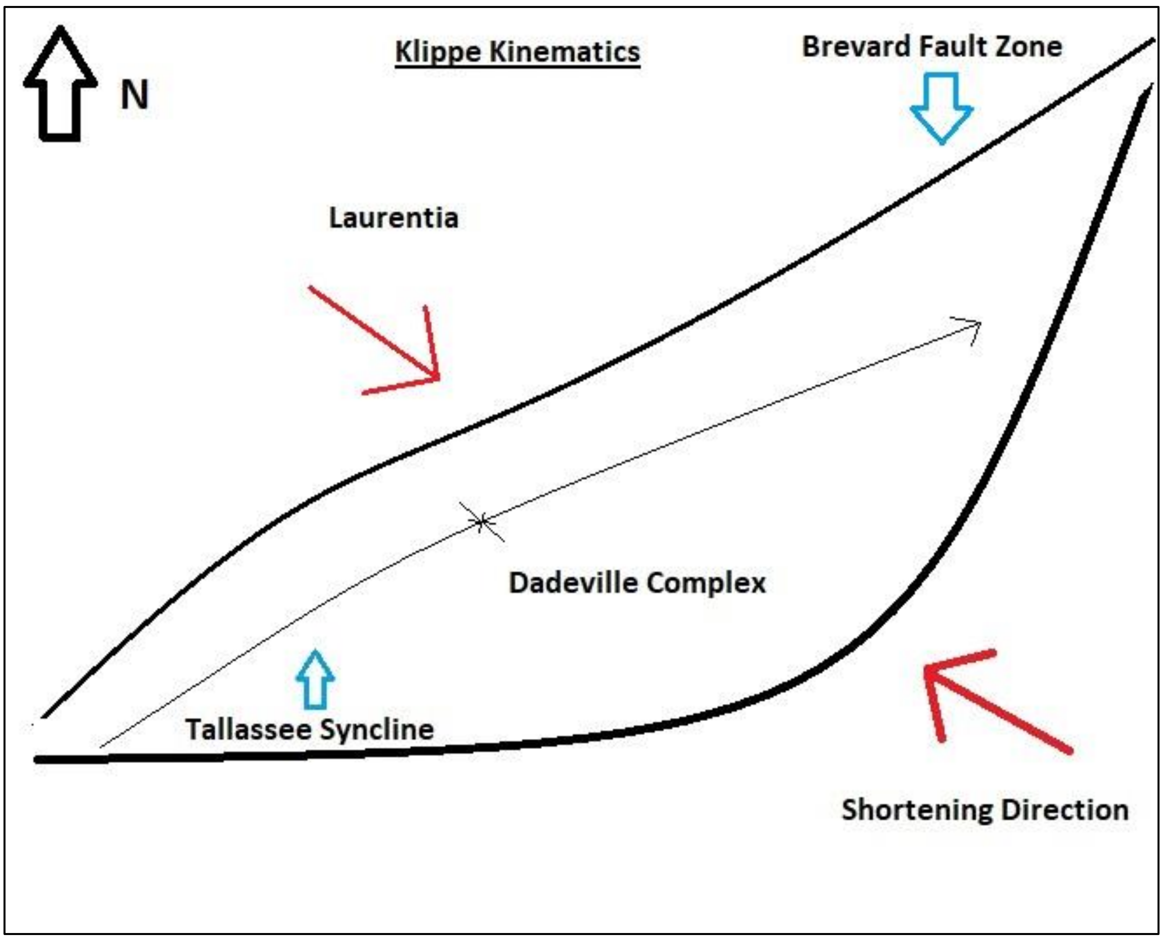

Figure 1.3

Simplified model illustration of klippe kinematics.

The purpose of this thesis is to study the Dadeville and Opelika Complexes and their contact, the Stonewall Line, within the Cusseta quadrangle, Chambers County, Alabama as part of an EDMAP project in coordination with the USGS and the Geological

Survey of Alabama. Outcrop mapping, taking oriented samples, and thin section analysis was conducted from data and samples collected determining the type and magnitude of strain along with kinematics present and style of movement they correspond to. This study has implications for the role and processes of terrane accretion during mountain building.

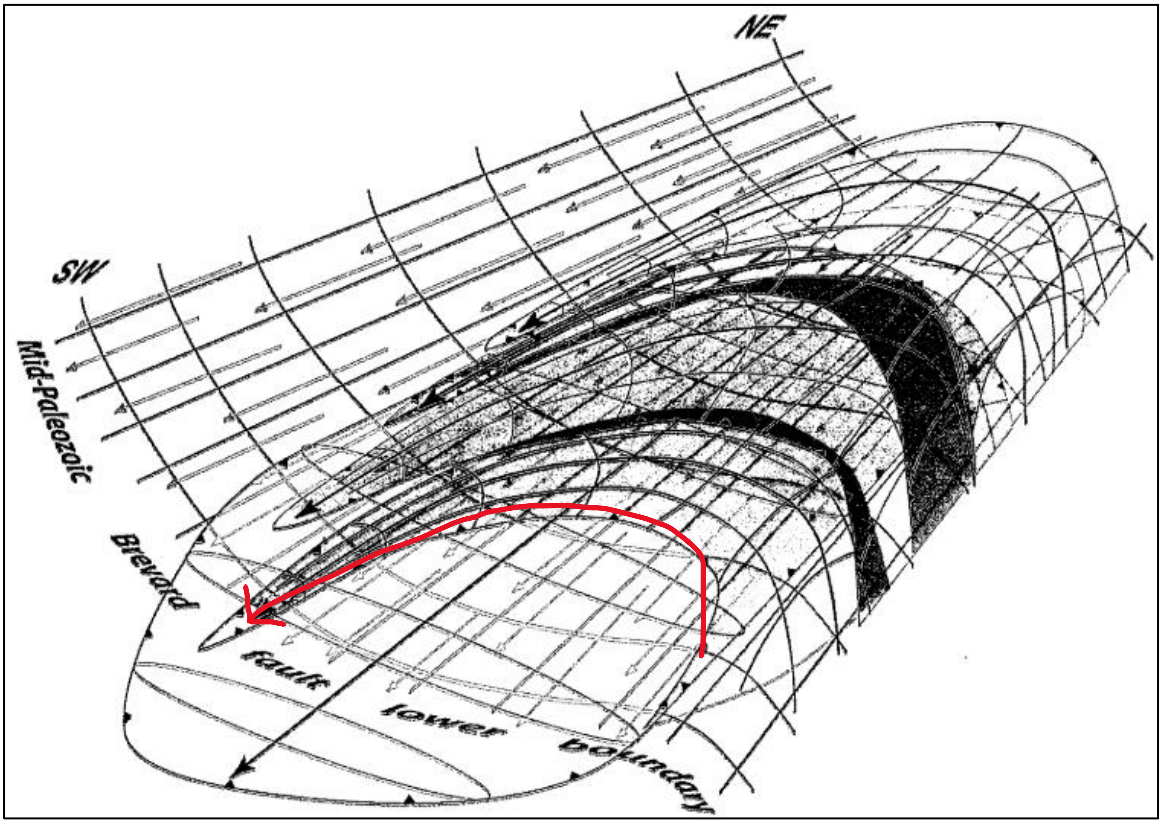

Figure 1.4

Illustration of channel flow (modified from Hatcher and Merschat, 2006). Red arrow indicates trend of lineations and direction of flow.

CHAPTER II - GEOLOGIC HISTORY

The Alabama Appalachians represent the southwestern most exposures of the Appalachian orogen and comprise part of the Alabama promontory of the Laurentian-Iapetus margin, plus terranes that have accreted to this margin during the growth of the Appalachians. Lithotectonic block subdivisions have been made in the Alabama Appalachians on the basis of major fault zones and/or lithological contrast between adjacent blocks (Drummond et al., 1997).

The Dadeville Complex and Opelika Complex are interpreted to originate from the Taconian orogeny (Ordovician Period). The southern extent of the Taconian orogeny in the IP has been poorly constrained due to lack of structural and mineral kinematic data from accreted terranes during that time. Terrane distinctions can be found in the northern portions of the Inner Piedmont in northeast Georgia and the Carolinas, but clear evidence has not been found in the southern most sections within Alabama and southwest Georgia (Merschat et al., 2005; Hatcher and Merschat, 2006; Ma et al., 2019).

The Taconian orogeny is best recorded in the southern Appalachians by K-Ar/Ar-Ar dating (Steltenpohl and Kunk, 1993), and sedimentary sequences containing bentonites from the foreland, documenting evidence of Middle to Upper Ordovician volcanism when Laurentia and peri-Gondwanan/Gondwanan terranes started to accrete, forming the Dadeville back-arc system (Ma et al., 2019). High-grade metamorphism is found in the western Blue Ridge province, bimodal volcanism and granulite-eclogite metamorphic facies in the eastern Blue Ridge province, and granitic plutonism within the Inner Piedmont (Merschat et al., 2005; Hatcher and Merschat, 2006; Tull et al., 2018; Ma et al., 2019).

The Acadian orogeny is best described as the collisional event that occurred between the Eastern Blue Ridge margin of Laurentia and the Inner Piedmont during the Early to Late Devonian Period. This is best recorded by the Acadian-aged synmetamorphic to late-metamorphic S-type granites that are prominent throughout the EBR and IP resulting from the peak metamorphic temperatures from crustal anatexis during that time. The inverted metamorphic gradient of the overlying sillimanite grade Dadeville Complex to the kyanite-staurolite grade Opelika Complex also suggests a collisional event occurred resulting in stacked thrust sheets (Drummond et al., 1997).

The Neoacadian orogeny is best described as the closure of the remnant Rheic Ocean basin (Cat Square terrane) between Laurentia and the approaching Carolina superterrane and resulting collision and magmatism during the Late Devonian Period through the Mississippian Period (Hatcher et al., 2007). The Alleghanian orogeny is best described by the closure of the Theic Ocean basin and collision of Gondwana to Laurentia during middle Carboniferous to late Permian Period forming the supercontinent Pangea (Huebner et al., 2017).

2.1 Structural Components

Shallow-dipping foliation and a stack of gently dipping crystalline thrust sheets characterize the Inner Piedmont. These thrusts are Type-F thrusts, which are lobate, plastic and fold-derived, with meso-fabrics that are penetrative, and which evolved beneath the ductile–brittle transition (Merschat et al., 2005; Hatcher and Merschat, 2006). It has been suggested that the Dadeville Complex is a fault-bounded synformal klippe feature, known as the Tallassee synform (Fig. 2.1) (Neilson and Stow, 1986; Farris et al., 2017; Tull et al., 2018). The northern extent of the Dadeville Complex structurally overlies the Ordovician-aged Jacksons Gap Group and is bounded by the Katy Creek Fault (low-temp overprint of the Neoacadian Brevard FZ), while bounded by the Stonewall Line fault system to the south. The Katy Creek and Stonewall Line fault system is suggested to cut through the older metamorphic features, which constrained the P-T conditions (3-10 kbar & 500-800°C) of the peak metamorphism (Tull et al., 2018).

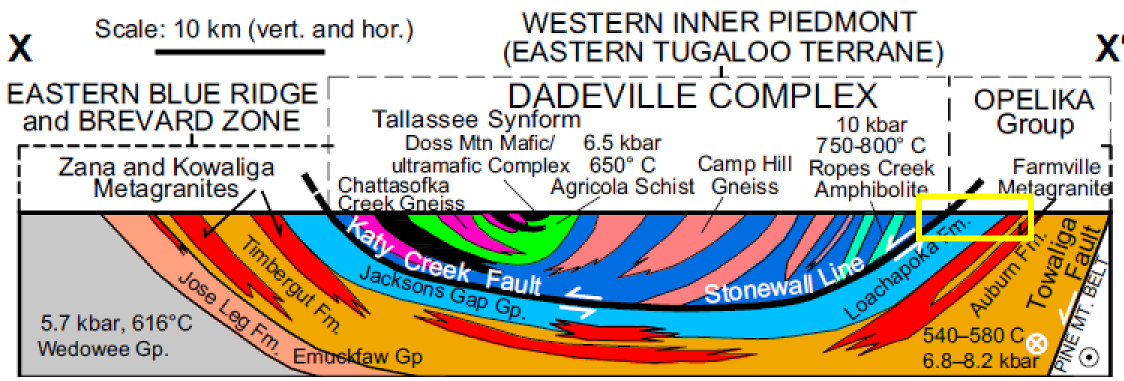

Figure 2.1

Cross section through the Dadeville Complex (modified from Farris et al., 2017 & Tull et. al., 2018). Area of focus outlined in yellow.

2.2 Lithology

Lithologically, the Dadeville Complex is comprised of younger meta-sedimentary rocks, while meta-volcanic/plutonic rocks comprise the older core (Bentley and Neathery, 1970; Sears et al., 1981; Neilson and Stow, 1986; Ma, et al, 2019). The various units comprising the Dadeville Complex are the Agricola Schist, Camp Hill Gneiss/Granite, Chattosofka Creek (Rock Mills) Gneiss, Ropes Creek Amphibolite, and other mafic/ultramafic rock suites, referred to by Neilson and Stow (1986) as the Doss Mountain and Slaughters Gabbro. The most structurally pronounced units within the Dadeville Complex are the Agricola Schist, Camp Hill Gneiss, and Ropes Creek Amphibolite (Sears et al., 1981; Steltenpohl, 1993).

Some authors suggest that the Waresville Formation (Bentley and Neathery, 1970), the Waverly Gneiss, and the Zebulon Formation (Sears et al., 1981) are part of the Ropes Creek Amphibolite rather than being designated as separate units (Farris et al., 2017). The lithologic units most important to this thesis are units just north of the Stonewall Line within the Dadeville Complex which include the Ropes Creek Amphibolite, Waverly Gneiss, and Agricola Schist and south of the Stonewall Line within the Opelika Complex which include the Loachapoka Schist and Farmville Metagranite, all within the Cusseta quadrangle (Fig. 2.2).

Dadeville Complex	Agricola Schist
	Waverly Gneiss
	Ropes Creek Amphibolite
	Stonewall Line
Opelika Complex	Farmville Metagranite (Bottle Granite) (Intrudes Auburn Gneiss and Loachapoka Schist)
	Loachapoka Schist
	Auburn Gneiss

Figure 2.2

Generalized stratigraphic column of the geologic units within the Cusseta quadrangle.

The structurally lowest section within the Dadeville Complex (Ropes Creek Amphibolite) is interpreted to be roughly 9km thick and is strongly foliated amphibolite with alternating layers of plagioclase feldspar and hornblende amphibole. Some interlayers of dacitic metatuff and metasedimentary rocks are contained within the Ropes Creek unit as well. The protolith of the Ropes Creek Amphibolite was dominantly tholeiitic basalt (partial melt of olivine rich basalt produced by decompression melting) (Neilson and Stow, 1986; Farris, et al., 2017).

The Agricola Schist lies above the Ropes Creek Amphibolite and has an average thickness of 1km. Its foliation is defined by cm-to-m layering of metapelitic/quartzofeldspathic composition. Some layering, no thicker than 1m, of amphibole can be found throughout. The protolith for the Agricola Schist is interpreted to be meta-turbiditic (Farris, et al., 2017; Tull et al., 2018).

Lithologically, the Opelika Complex is comprised of the Loachapoka Schist, Auburn Gneiss, and Farmville Metagranite (informally Bottle Granite; Bentley and Neathery, 1970; Osborne et al., 1988) (Fig. 2.2). The Opelika Complex contains mostly amphibolite grade metasedimentary rocks with only minor amounts of mafic rock. The southern extent of the Opelika Complex is bounded by the mylonitic Towaliga Fault Zone.

The Loachapoka Schist is kyanite/sillimanite bearing schist with a metapelitic protolith containing interlayered quartzites and rare, thin amphibolite (Goldberg and Steltenpohl, 1990). The quartzite layers are discontinuous into Georgia and informally known as the Saugahatchee quartzite (Sears et al., 1981). The Loachapoka Schist is intruded by felsic pegmatites and numerous bodies of Farmville Metagranite (Bottle Granite) (Goldberg and Steltenpohl, 1990). Poikiloblastic textures of garnet can be found throughout the Loachapoka Schist.

The Farmville Metagranite is a series of quartz dioritic plutons consisting of quartz, alkali and plagioclase feldspar, biotite, and muscovite, with minor constituents of garnet and epidote (Goldberg and Steltenpohl, 1990). The Farmville Metagranite intrudes the Auburn Gneiss and the overlying Loachapoka Schist, but not rocks structurally above the Opelika Complex (Sears et al., 1981; Goldberg and Steltenpohl, 1990). This unit is locally high strained and polydeformed, as exhibited by dominant (S1) fabrics visible in quartz, feldspar, and biotite (Goldberg and Steltenpohl, 1990).

The rocks of the Inner Piedmont are pervasively migmatitic, except along the flanks. P–T estimates range from 500–800 ^{o}C and 3–7 kbar (Merschat, 2005), and some ranges to 10 kbar for the basal contact of the Ropes Creek Amphibolite (Drummond et al., 1997; Tull et al., 2018). Single continuous garnet zoning profiles and an increase in temperature from garnet cores to rims from both the western and eastern IP indicate that the IP underwent one progradational amphibolitic/granulite grade metamorphic event (Merschat et al., 2005), and at least two retrogradational events (Goldberg and Steltenpohl, 1990). Retrograde greenschist facies assemblages in both the Dadeville and Opelika Complexes resulted from Alleghanian reactivation of the Brevard Fault Zone (Goldberg and Steltenpohl, 1990; Merschat et al., 2005).

The Dadeville Complex metamorphic grade is amphibolite to low granulite facies, indicating 700-800^{o}C and 8-10 kbar, which is evidenced within the Ropes Creek Amphibolite and Agricola Schist (Drummond et al., 1997). The high-grade metamorphism is indicated by sillimanite-bearing ductile shear zones within the Dadeville Complex (Dadeville and Agricola shear zones) that is suggested to exhibit subhorizontal, northeast-trending stretching lineations postdating the peak metamorphism, as indicated by overprinting relationships of mineral assemblages (Bittner and Neilson, 1990; Drummond et al., 1997, Ma et al., 2019).

The Opelika Complex has a history of two tectonothermal deformational episodes with the amphibolitic progradational episode occurring during the Upper Devonian-Lower Carboniferous Periods, and the second episode of greenschist retrogression during the Upper Carboniferous. The first (D1) phase is suggested to have produced kyanite bearing amphibolitic metamorphism (~620^{o}C & 8.2 kbar) before retrograding at a lower amphibolite facies (~540-580^{o}C & 6.8-8.2 kbar) (Goldberg and Steltenpohl, 1990; Steltenpohl and Kunk, 1993; Drummond et al., 1997). The principal amphibolite phase is responsible for the (S1) fabric foliation in the Auburn Gneiss and Loachapoka Schist (Goldberg and Steltenpohl, 1990; Drummond et al., 1997). Garnet zoning profiles support the earlier retrogression. The second episode (D2) has been suggested to have produced a greenschist facies retrogressional Alleghanian overprint of the earlier amphibolite facies, which caused extensional crenulation cleavage that formed (S2) to deform the (D1) fabrics (Goldberg and Steltenpohl, 1990).

CHAPTER III - METHODS

The research plan was to create a detailed geologic map of the Cusseta quadrangle delineating structural, mineralogical, and petrological characteristics and patterns, as well as the shear type and direction, and kinematics of structural components. Stereonets (Allmendinger et al., 2012; Cardozo and Allmendinger, 2013), and thin section analysis have been completed to help understand the kinematics within and between the Dadeville and Opelika Complexes and the Stonewall Line. This project considered both the regional and microscopic level, allowing for the different kinematic models of Dadeville and Opelika Complex formation and evolution to be better constrained.

3.1 Geologic Mapping

Strike, dip, plunge, and trend measurements of mineral foliations and lineations were collected from multiple trips to the area. A handheld GPS system was used in the field for precise outcrop location to produce the most up-to-date map of the Cusseta quadrangle. The Cusseta quadrangle was divided into four sections, one section for each trip, starting in the SE corner and working clockwise. Multiple topographic maps made with ArcGIS Pro, at both larger and smaller scales, were used to plot outcrop locations within the quadrangle. Original maps from previous mapping excursions and the current geologic state map were used as a guide to plan investigation.

Outcrops were found by driving along all roads in both directions within the Cusseta quadrangle, looking for road cuts, power lines, bridges, ditches, and other fluvial drainage systems that were prime areas for potential outcrops. While driving, a person on each side of the vehicle carefully scanned for any semblance of rock. Most outcrops are small, weathered, and surrounded by soil and roots. Once at these areas, surveying was then done on foot to try to locate outcrops of good quality unaffected by anthropomorphic and weathering processes. Timber logging created clear cuts throughout sizeable sections of the quadrangle, which allowed the normally densely vegetated areas to be scouted efficiently and effectively.

All maps were digitized using ArcGIS Pro for the completed version of the geologic map. A topographic map used to plot mapping data, and scans of tracing paper with sketched out map patterns within the Cusseta quadrangle were scanned and georeferenced into ArcGIS Pro. ArcGIS Pro was then used to create new polygons delineating inferred contacts and mapping symbols (e.g., strike and dip of foliations, trend and plunge of lineations) between the units, and any other structural feature present (Cusseta Synform) within the quadrangle. USGS symbols were used to plot mineral foliation and lineation orientations. “Right-Hand Rule” strike, dip azimuth, and degree of dip fields were created to properly orient foliation symbols and labeling of degree of dip. Creating lineations were similar to foliations by constructing trend and plunge fields to correctly orient their position to map.

3.2 Petrographic Analysis

Multiple samples were collected from the field for analysis. Oriented samples are taken by measuring the foliation and lineation, if obvious, and then measuring the orientation of a relatively planar face, sometimes the same as the mineral foliation plane or a fracture. The sample is marked along the measured plane with a strike and dip map symbol that illustrates the direction of strike and the dip plane following the “Right-Hand Rule” method with an arrow pointing towards the strike. This orientation allows samples to be re-oriented in the lab and structures such as lineations to be measured and placed back into the geographic reference frame once back in the lab, since lineations were not always obvious in the field.

The samples were cut parallel to the lineation vector and perpendicular to the foliation plane to help constrain the axis of maximum elongation and shear, so called the kinematic plane. The cut face was marked by wax pen to show where the cut was taken from the slabbed rock and to help orient the future thin section back to the rock. Thin sections were made from these samples and analyzed for any shear movement, lineation, foliation, and mineral assemblages. This has helped to determine the presence of polydeformed fabrics, kinematics, and other metamorphic textures like mineral assemblage and grain size. Mineral percentages determined in thin section were completed by approximate modal analysis using a percent mineral abundance chart (Perkins and Henke, 2003).

3.3 Kinematics

All structural data collected in the field and determined in the thin sections were plotted on stereonets to complete kinematic analysis. Kinematics determined in thin section was completed by looking for delta/sigma clasts, S-C fabrics, and shear direction within the mineral assemblage. Thin sections were then oriented to the sample collected from the field outcrop to determine the shear type and direction and then projected to the region. This was done by taking the cut section, placing it back to the oriented rock sample and using the shear direction determined by delta/sigma clasts and S-C fabrics under microscope to determine the correct shear type and direction relative to the sample and geographic north.

CHAPTER IV - RESULTS

Throughout this section, rock distribution, petrographic analysis, and geologic mapping of the Dadeville and Opelika Complexes within the Cusseta quadrangle will be presented.

4.1 Rock Distribution

Roughly ninety-four percent of the area of the Cusseta quadrangle is encompassed by the Dadeville Complex, which includes the Ropes Creek Amphibolite (RCA), Waverly Gneiss, and a small section of the Agricola Schist. The Opelika Complex comprises the other six percent by area of the quadrangle, which includes the Loachapoka Schist and the Farmville Metagranite in the southeastern corner of the quadrangle. The boundary between the two complexes, the Stonewall Line, is roughly parallel to Highway I-85.

Seventy-five outcrop locations were observed during trips to study the Cusseta quadrangle (Fig. 4.1). Of those seventy-five, seven were outside of the quadrangle close to the border (Loc. 1, 2, 3, 17, 20, 34, and 51), with the remaining sixty-eight locations being within the boundary. Outcrop and rock/sample quality and availability varied greatly across the quadrangle with some very small outcrops (~1 m^2 exposed), large areas lacking outcrops, and some outcrops being completely replaced as saprolite. Road access was overall good, but some areas of the quadrangle, namely most stream systems and private land, were not accessible. Some units were more affected by alteration than others; for example, within the Ropes Creek Amphibolite, many outcrops were weathered into an orange-colored clay saprolite. In many outcrops, only remnant bands of feldspar and/or quartz are left to indicate the foliation plane for the saprolitic sections of the RCA.

All outcrop locations designated as the Waverly Gneiss were consistent in quality, with the mineral assemblage for these outcrops containing mostly quartz and feldspar and lesser amounts of amphibole. The one outcrop designated as the Agricola Schist (Loc. 55) was of decent quality, being micaceous at outcrop but difficult to distinguish foliation at that scale.

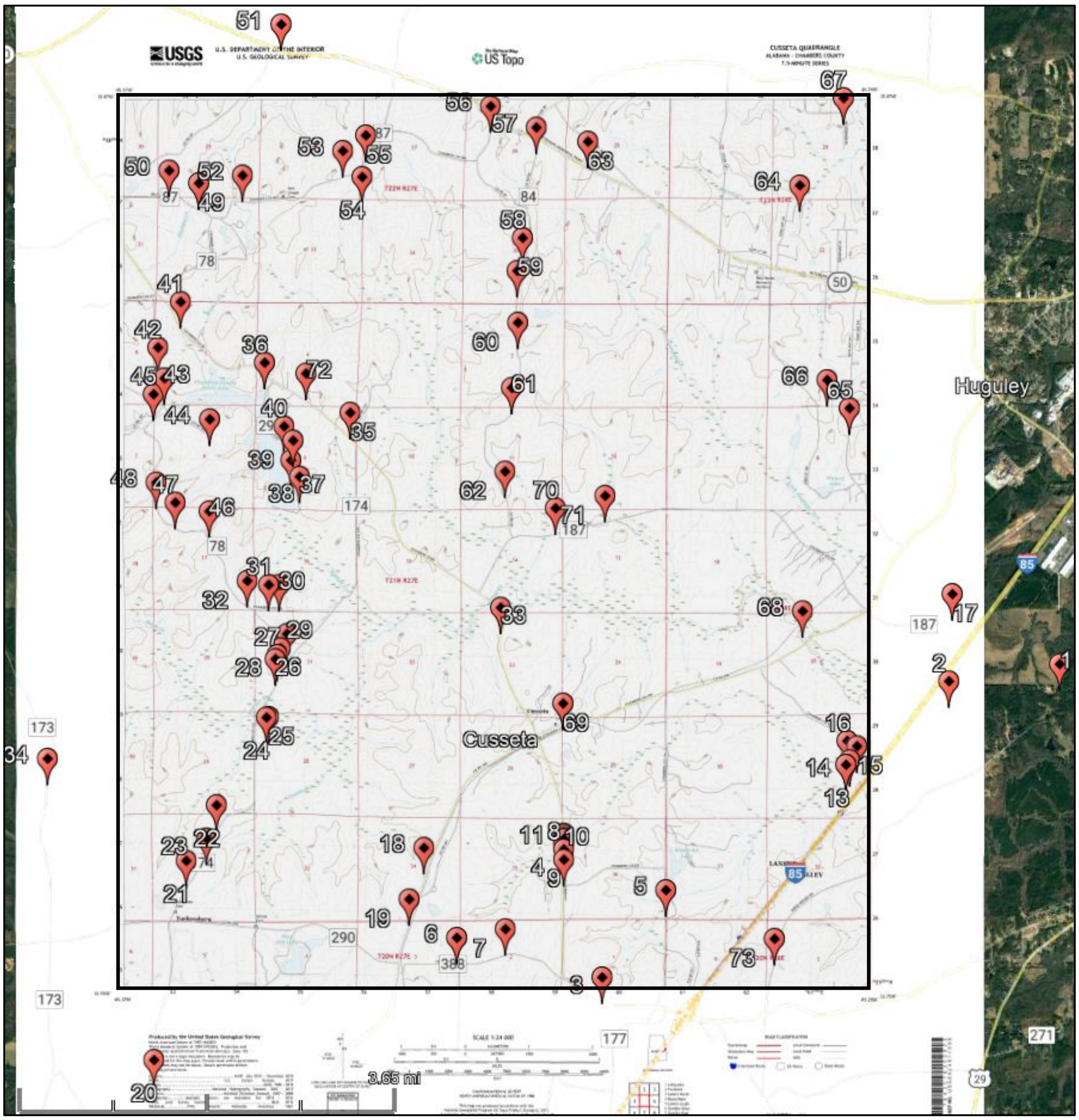

Figure 4.1

Outcrop locations within and around the Cusseta 7.5' Quadrangle. Image from Google Earth Pro with USGS topo overlay.

With such a small area of Opelika Complex within the SE section of the quadrangle, only five outcrops are documented within the boundary. Of these five, four are within the Loachapoka Schist (Loc. 13-16) and the other (Loc. 73) is within the Farmville Metagranite. Outcrops within the Opelika Complex were difficult to find. The four outcrops within the Loachapoka Schist are all within a quarter mile radius of each other and in a section that had recently been clear cut for timber on Chambers Co 529. Two of these outcrops (Loc. 13 & 14) are a garnet muscovite schist, the third is a garnet sillimanite muscovite schist (Loc. 16), and the last, is a small migmatized section (Loc. 15). All outcrop locations were of good sample quality. The outcrop location within the Farmville Metagranite was a high-quality outcrop with well-defined mineral foliation planes determined from small amounts of biotite present.

Outcrops found within the Cusseta quadrangle were designated as either having a felsic or mafic protolith composition. This distinction was made by the mineral assemblages found in both hand sample and thin section. Samples with felsic protoliths contain primarily quartz and feldspar, while the samples with mafic protoliths contain a large component of dark minerals, like hornblende and biotite. Seventy-three percent of outcrop locations documented within the Cusseta quadrangle have mafic protoliths, with twenty-seven percent of outcrops having felsic protoliths.

Seventy-nine percent of the outcrop locations within the Dadeville Complex are classified as the Ropes Creek Amphibolite, including locally migmatized zones found in the east-central section and southwest section of the quadrangle. One outcrop location within the Cusseta quadrangle and Dadeville Complex (Loc. 55) is from a metasedimentary protolith and has a significantly different mineral assemblage compared to outcrops denoted as the RCA. This outcrop contains a high percentage of chlorite and pyroxene with lesser amounts of amphibole and is denoted as the Agricola Schist for this study but compositionally seems better related to the Waresville Schist. All felsic protolith outcrop classifications within the Dadeville Complex are associated with the Waverly Gneiss and make up the remaining twenty-one percent of the outcrops. The remaining nine percent of the felsic protolith composition within the Cusseta Quadrangle is designated to the Loachapoka Schist and Farmville Metagranite associated with the Opelika Complex. Refer to Appendix A Table A.1 for mineral assemblage composition and associated data found in thin section for the following section on petrographic analysis.

4.2 Petrographic Analysis

4.2.1 Opelika Complex: Loachapoka Schist

Most well-exposed outcrops found within the Cusseta quadrangle and the Opelika Complex are of the Loachapoka Schist. Outcrops denoted as the Loachapoka Schist are all similar in mineral assemblage, being highly micaceous (mostly muscovite and some biotite) with other minerals within the assemblage being alkali feldspar, quartz, and lesser amounts of sillimanite and garnet (Fig. 4.2). Large boudinaged quartz veins (~10-15cm) are present at locations 13 and 14. These veins, possibly related to the migmatized zone at location 15, contain finer-grained garnet as compared to the host rock. Textures of the Loachapoka Schist are primarily fine- to medium-grained, apart from the micaceous minerals that are medium- to coarse-grained, with increased grain size approaching the Stonewall Line, where micaceous minerals grew in excess of 10+cm.

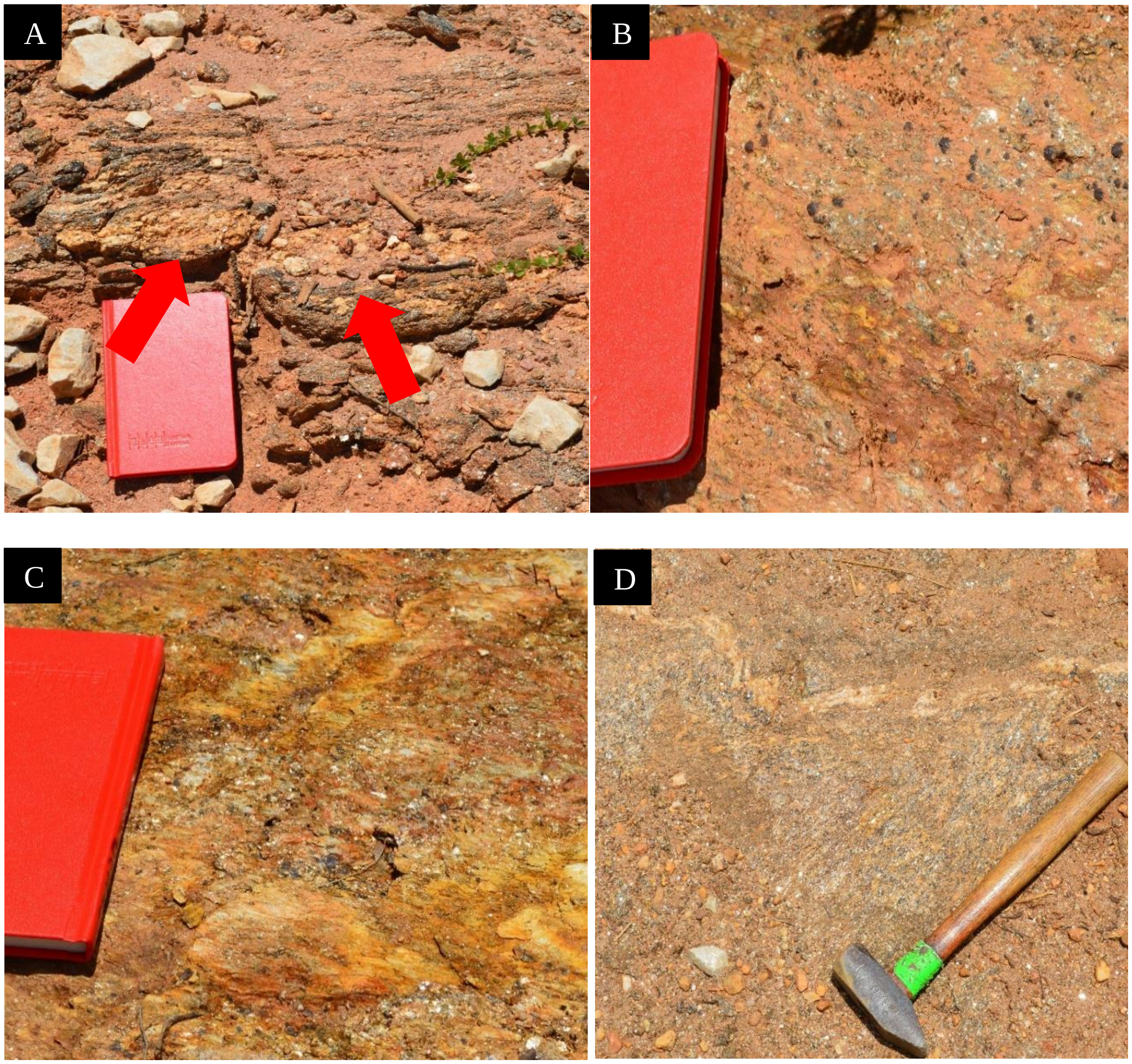
A
B
C
D

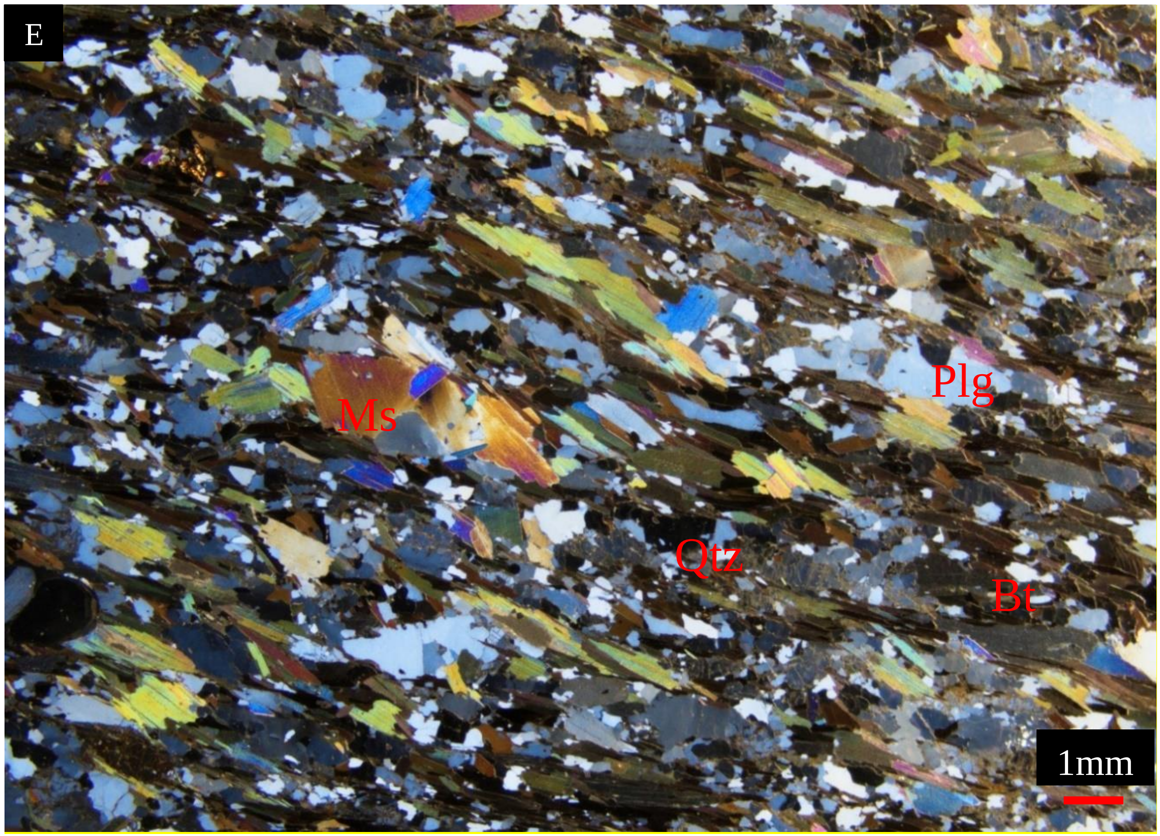
E
Ms
Plg
Qtz
Bt
1mm

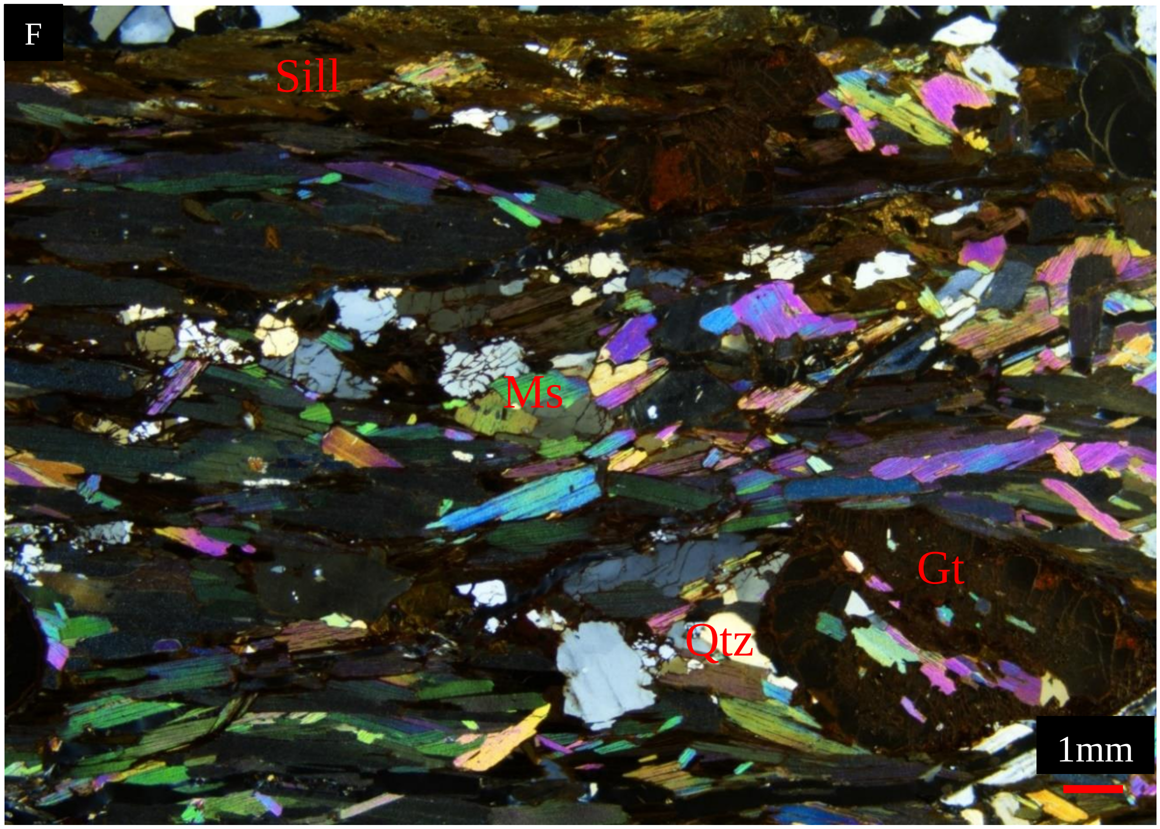

Figure 4.2

Outcrop locations 13-16 within the Loachapoka Schist (Opelika Complex) (Quartz=Qtz, Biotite=Bt, Muscovite=Ms, Alkali feldspar=Alk, Plagioclase=Plg, Amphibole=Amph, Pyroxene=Px, Kyanite=Ky, Sillimanite=Sill, Chlorite=Chl, Garnet=Gt). **A.)** Boudinaged quartz veins (red arrows) found at locations 13 and 14. **B.)** Garnet schist found throughout locations 13-16. **C.)** Sillimanite bearing schist at location 16. **D.)** Migmatized zone at location 15. **E.)** Thin section from sample OCC-CB-04 at location 13. Quartz is extinct in this image **F.)** Thin section from sample OCC-CB-07 at location 16.

Sillimanite is found in the highest concentrations closest to the Stonewall Line (Loc. 16) in the Loachapoka Schist with decreasing amounts further south. A small localized migmatized section containing garnet (Loc. 15) from a muscovite-rich protolith is documented in the Loachapoka Schist. This was the only migmatized section found in the Opelika Complex within the Cusseta quadrangle.

4.2.2 Farmville Metagranite

The one outcrop location (Loc. 73) documented as the Farmville Metagranite in the Cusseta quadrangle is dominantly comprised of alkali feldspar and quartz, with lesser amounts of plagioclase feldspar, biotite, and muscovite (Fig. 4.3). Texturally, the mineral assemblage for the Farmville Metagranite is fine-grained, except muscovite mica, which is medium-grained, similar to outcrops in the Loachapoka Schist. Mineral assemblage and percentages of this Farmville Metagranite outcrop at location 73 show a similarity to the Waverly Gneiss of the Dadeville Complex.

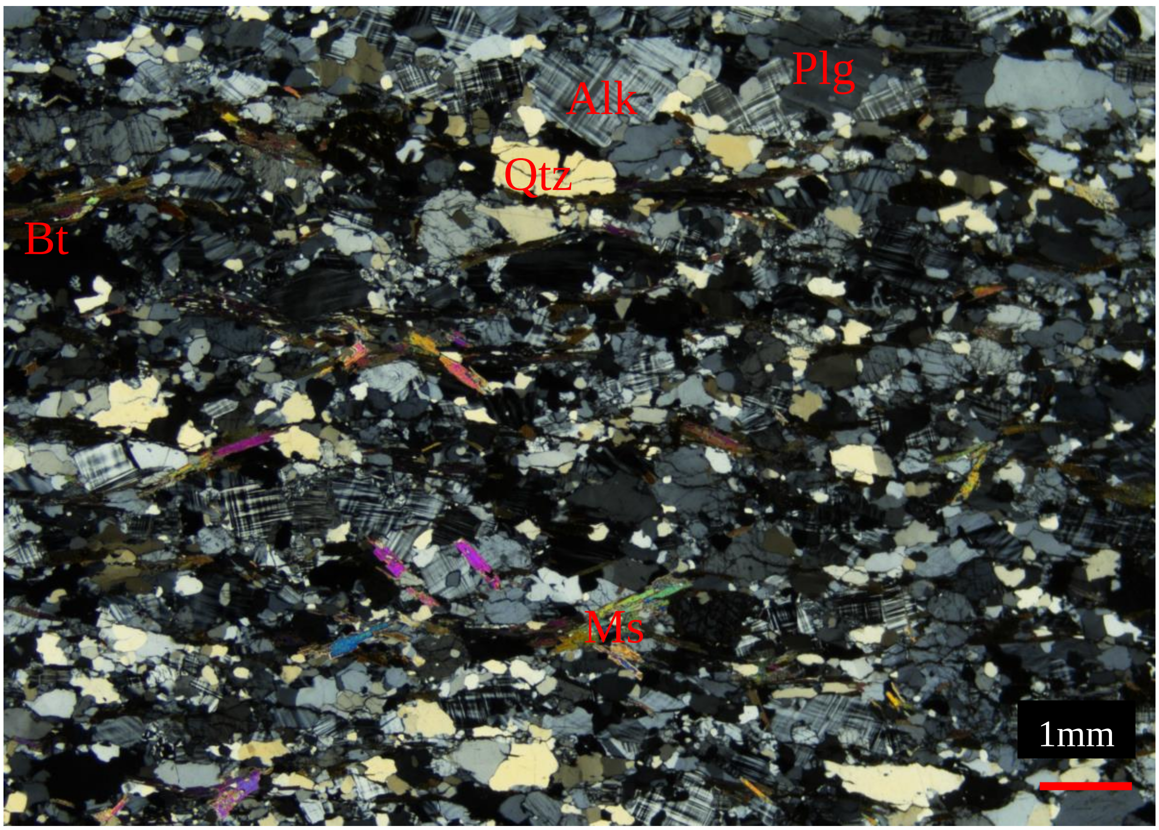

Figure 4.3

Thin section from sample OCC-CB-08 at location 73 (Quartz=Qtz, Biotite=Bt, Muscovite=Ms, Alkali feldspar=Alk, Plagioclase=Plg, Amphibole=Amph, Pyroxene=Px, Kyanite=Ky, Sillimanite=Sill, Chlorite=Chl, Garnet=Gt).

4.2.3 Dadeville Complex: Ropes Creek Amphibolite

The Ropes Creek Amphibolite is a strongly foliated amphibolite with alternating layers of plagioclase feldspar and hornblende amphibole with a protolith of tholeiitic basalt (Neilson and Stow, 1986; Farris, et al., 2017). Figure 4.4 A&B shows the variance of outcrop quality within the RCA. Samples collected from the field were mostly equigranular, sugary, and fined-grained, with a weakly defined foliation defined by the phases. Lighter colored minerals (quartz and feldspar) within the RCA define the plane of foliation in addition to the gneissic banding.

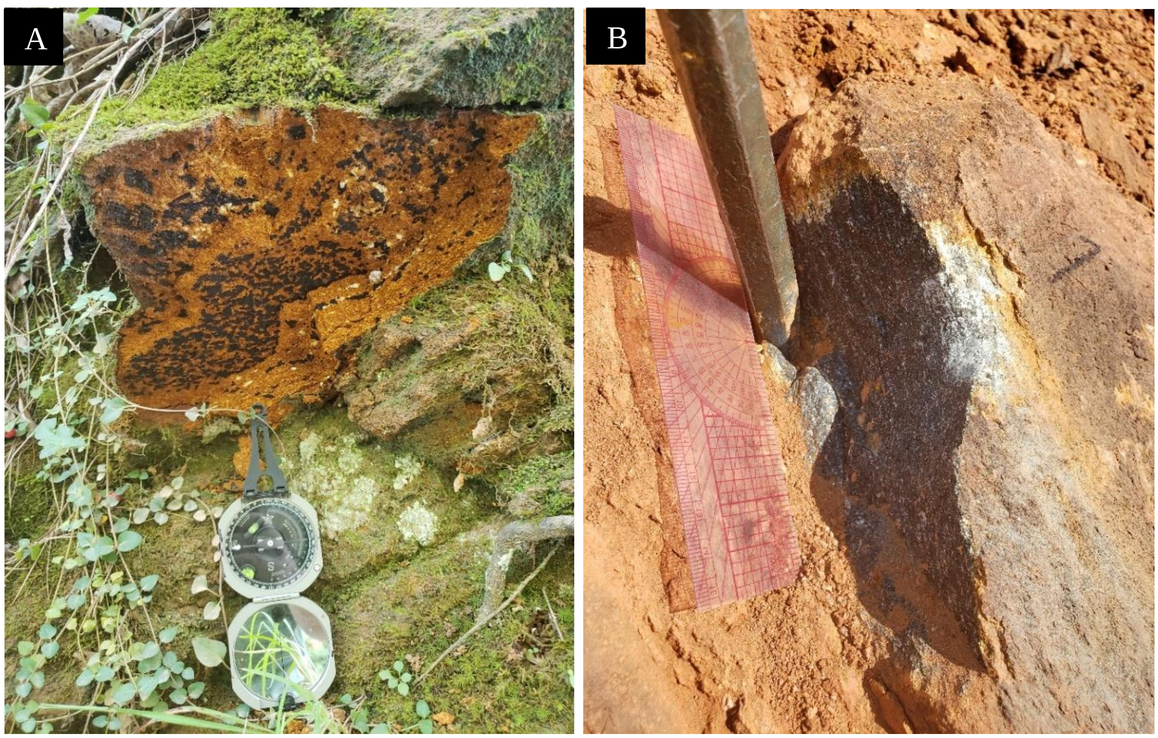

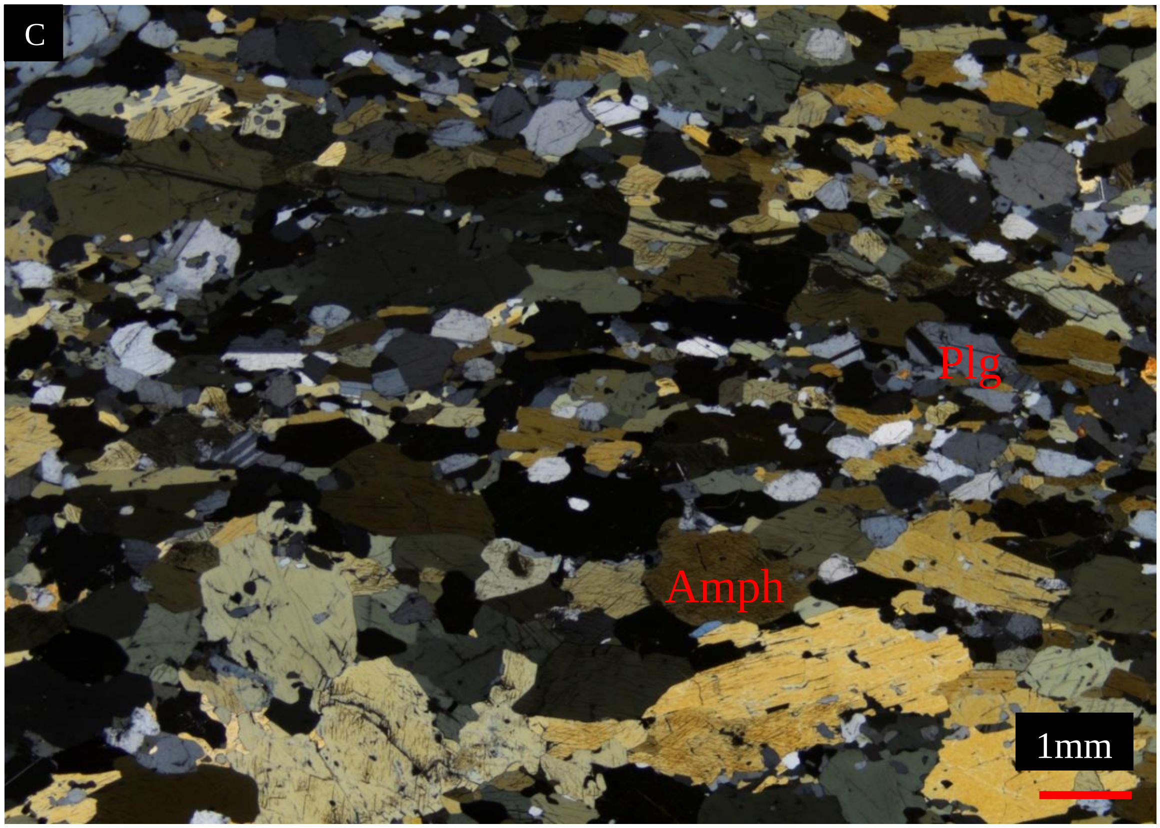

Figure 4.4

Outcrops in the RCA showing differences of quality. (Quartz=Qtz, Biotite=Bt, Muscovite=Ms, Alkali feldspar=Alk, Plagioclase=Plg, Amphibole=Amph, Pyroxene=Px, Kyanite=Ky, Sillimanite=Sill, Chlorite=Chl, Garnet=Gt) **A.)** Saprolitic section at location 20. **B.)** High quality outcrop at location 21 and sample DCC-CB-10. **C.)** Thin section of sample DCC-CB-10 from location 21.

In both the thin sections and hand samples, there is a dominant percentage of amphibole present throughout outcrops denoted as the RCA. No less than thirty percent of any sample collected in the RCA is comprised of amphibole, and in some samples, up to sixty percent. Other minerals found in these samples are plagioclase feldspar and to a lesser extent, quartz. In areas that were found to be migmatized in the west-central section of the quadrangle (Loc. 38, 40, 46-48), garnet is present in amounts no greater than ten percent and were of increased grain size at location 48, which is a migmatized pavement outcrop.

Actinolite veins are present at location 44 (Fig. 4.5). Mineral foliation was difficult to distinguish at this location and through hand-lens analysis, fine grained garnet seemed to be in the mineral assemblage, but not found in thin section. Location 44 was the only outcrop within the Cusseta quadrangle that contained a significant amount of pyroxene indicating this outcrop to be a gabbro instead of amphibolite. This outcrop is likely an intrusion of the Slaughters gabbro.

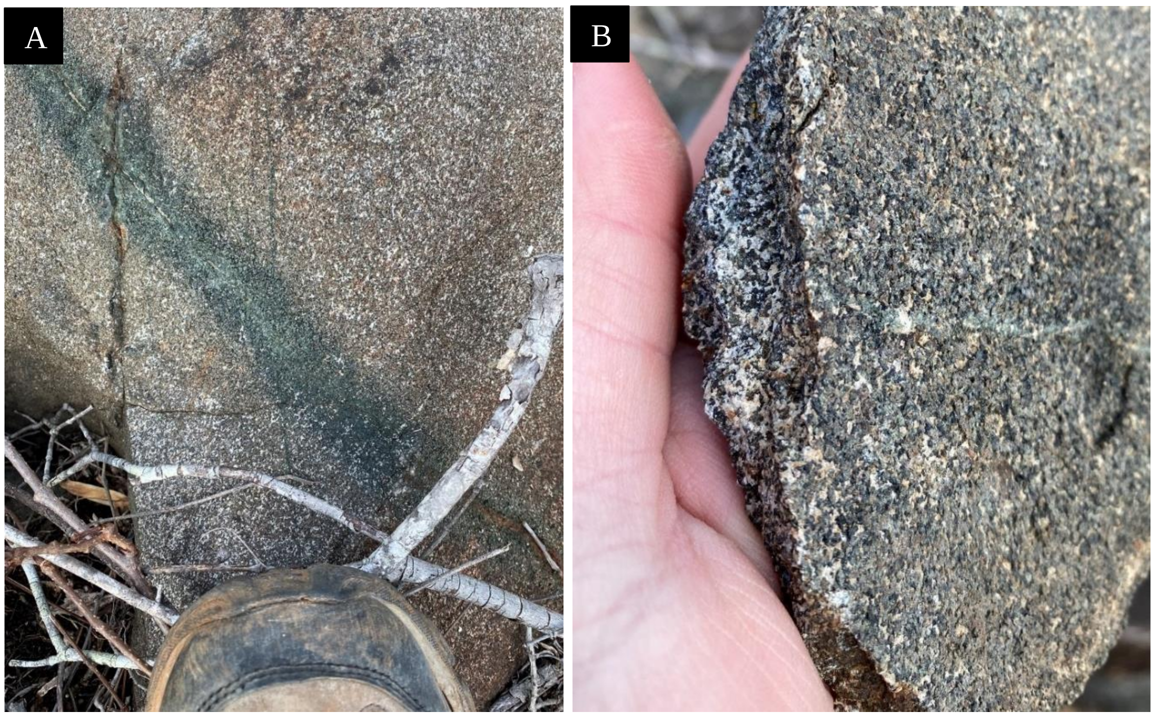

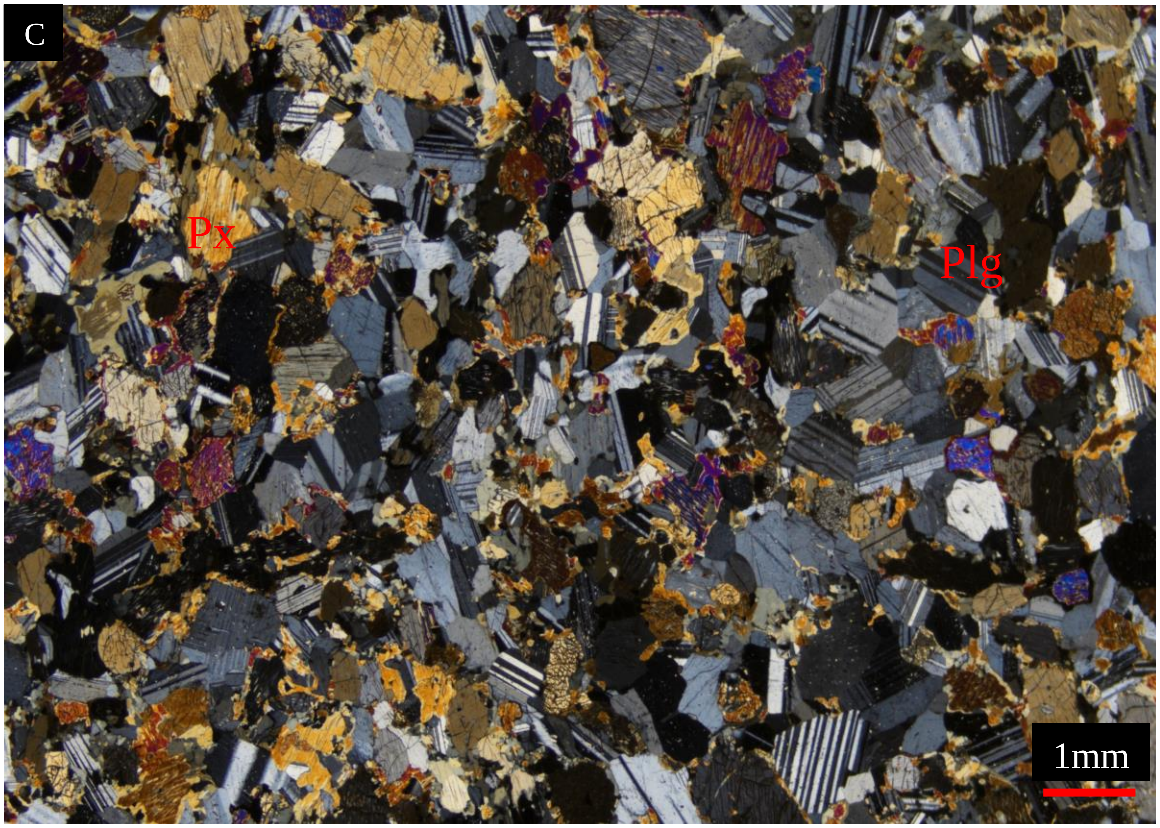

Figure 4.5

Location 44 and sample DCC-CB-25 (Quartz=Qtz, Biotite=Bt, Muscovite=Ms, Alkali feldspar=Alk, Plagioclase=Plg, Amphibole=Amph, Pyroxene=Px, Kyanite=Ky, Sillimanite=Sill, Chlorite=Chl, Garnet=Gt) **A.)** Actinolite vein. **B.)** Closer inspection of hand sample showing lack of defined foliation. **C.)** Thin section from sample DCC-CB-25.

4.2.4 Waverly Gneiss

Samples collected from the field and in thin section denoted as the Waverly Gneiss indicate a dominant mineral assemblage of quartz and feldspar with significantly lesser amounts of hornblende than the RCA (Fig. 4.6). The primary mineral assemblage found include plagioclase feldspar, alkali feldspar, quartz, and lesser amounts of mica and amphibole. The mafic minerals (hornblende and biotite) in the Waverly Gneiss define the foliation. Grain size from these samples show feldspar and quartz being mostly medium grained with mica and amphibole being fine grained. The Waverly Gneiss at both the outcrop scale and in thin section show slightly larger grain sizes than samples collected in the RCA.

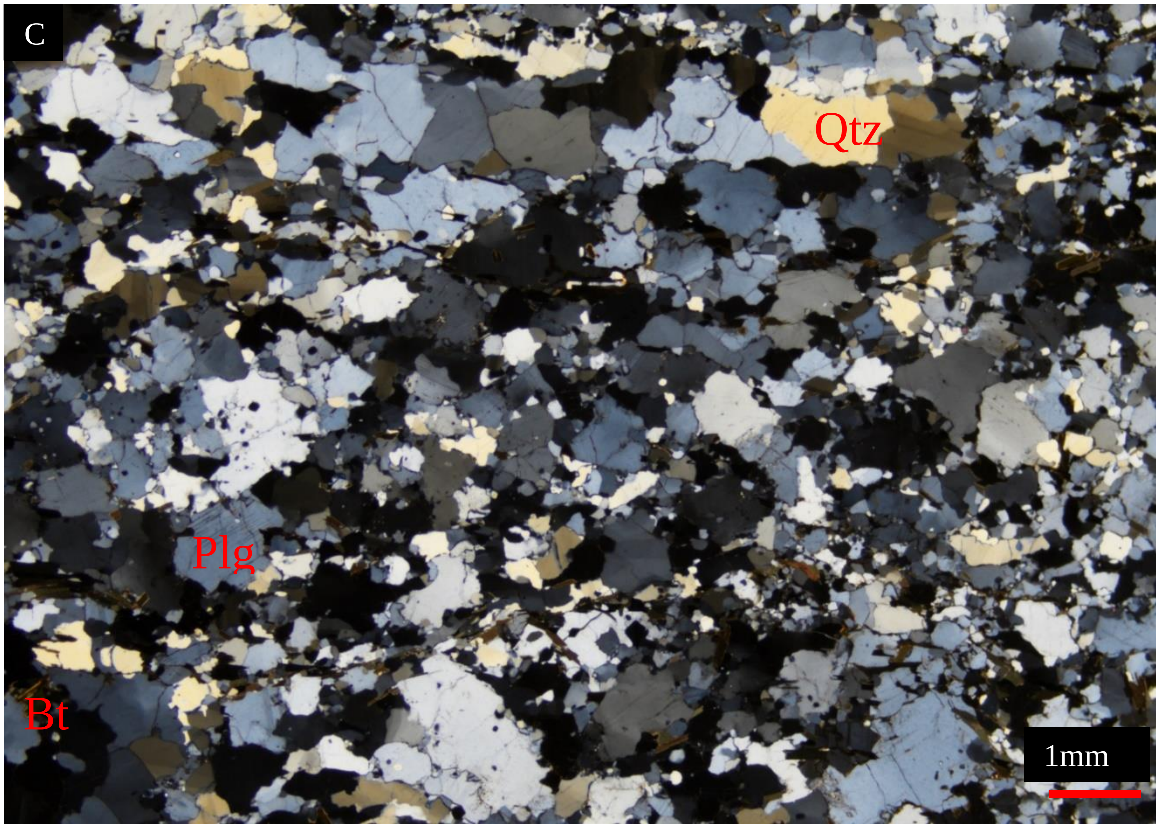

Figure 4.6

Outcrop location 36 of Waverly Gneiss near the entrance of Chambers County Public Lake. (Quartz=Qtz, Biotite=Bt, Muscovite=Ms, Alkali feldspar=Alk, Plagioclase=Plg, Amphibole=Amph, Pyroxene=Px, Kyanite=Ky, Sillimanite=Sill, Chlorite=Chl, Garnet=Gt) **A.)** Fellow USM geology graduate student standing in for scale. **B.)** A closer inspection of location 36, a leucocratic pod/vein in the bottom of the picture indicating the foliation plane and containing predominantly plagioclase feldspar and quartz with minor amounts of biotite. **C.)** Thin section from the same outcrop, sample number DCC-CB-20.

4.2.5 Agricola Schist?

One outcrop (Loc. 55) within the Dadeville Complex differed greatly in mineral assemblage compared to the rest of the outcrops within the Dadeville Complex. This outcrop is very micaceous at outcrop scale, but foliation is difficult to discern, while containing a great percentage of chlorite with lesser amounts of kyanite/sillimanite, pyroxene, and amphibole in thin section (Fig. 4.7). In thin section, kyanite and sillimanite crystals are medium grained, with the rest of the mineral assemblage being finer grained.

This outcrop resides close to a contact between the RCA and Waverly Gneiss and roughly 3km west of where the current Alabama geologic state map places this unit. This outcrop shows no similarities with lithology or mineral assemblages to what is currently defined as the Agricola Schist, the RCA, or the Waverly Gneiss. Mineral assemblage and composition show a relationship closer to the Waresville Schist than the Agricola Schist since the Waresville Schist is defined as a banded amphibolite interlayered with chlorite schist, chlorite amphibolite, chlorite-actinolite schist. Where a small limb of Agricola Schist is supposed to be, based on the current state geologic map, no lithologic changes or contacts were found in that area, suggesting that it instead is a continuation of the RCA and may not extend that far south within the quadrangle or that the outcrop limb was missed.

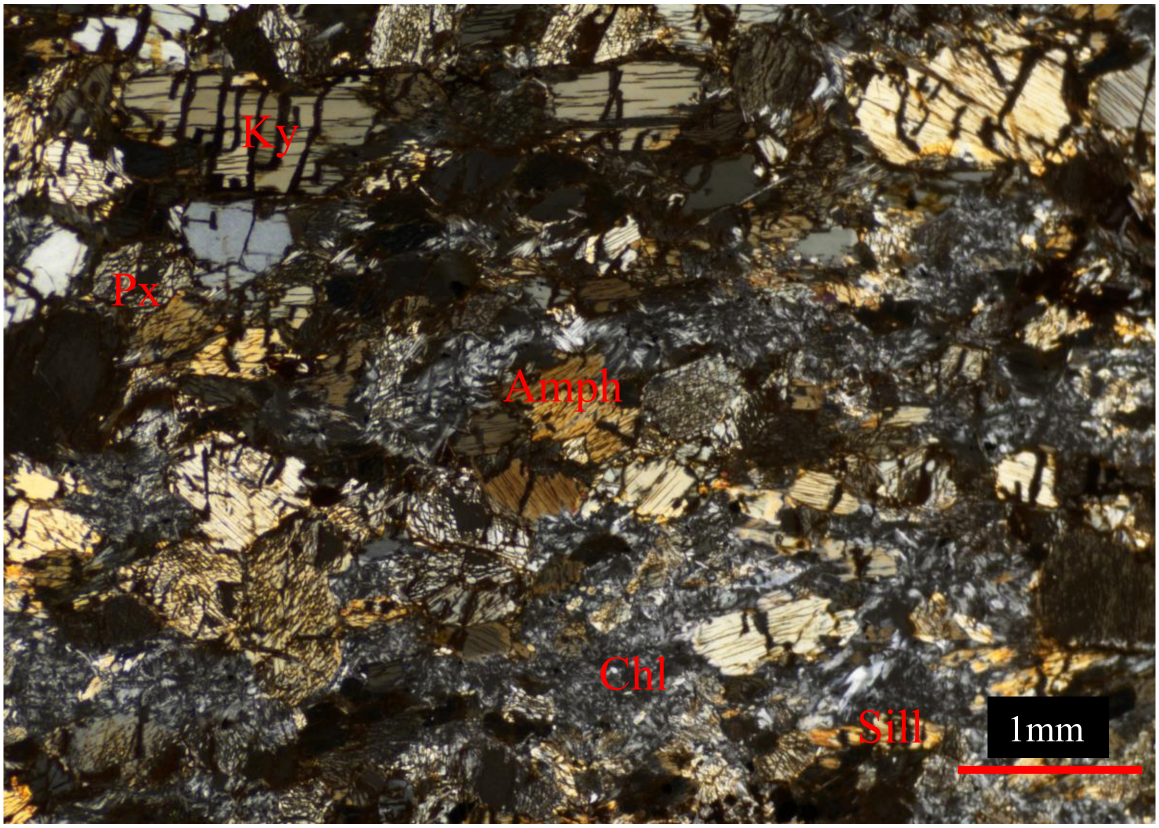

Figure 4.7

Thin section from sample from DCC-CB-29 at location 55 (Quartz=Qtz, Biotite=Bt, Muscovite=Ms, Alkali feldspar=Alk, Plagioclase=Plg, Amphibole=Amph, Pyroxene=Px, Kyanite=Ky, Sillimanite=Sill, Chlorite=Chl, Garnet=Gt).

4.3 Migmatized Dadeville Complex and Opelika Complex

Many areas within the Cusseta quadrangle contain migmatized zones of varying morphology. Most of the migmatized areas are found within the RCA of the Dadeville Complex (Loc. 35, 38, 40, 46-48, 68, and 72), apart from a small outcrop (Loc. 15) in the Opelika Complex. Further description of these migmatites will use terminology found in Sawyer (2008) to better describe both the composition, morphology, and tectonic implications associated with these features found throughout the Cusseta quadrangle.


A
B


C
D
E
F

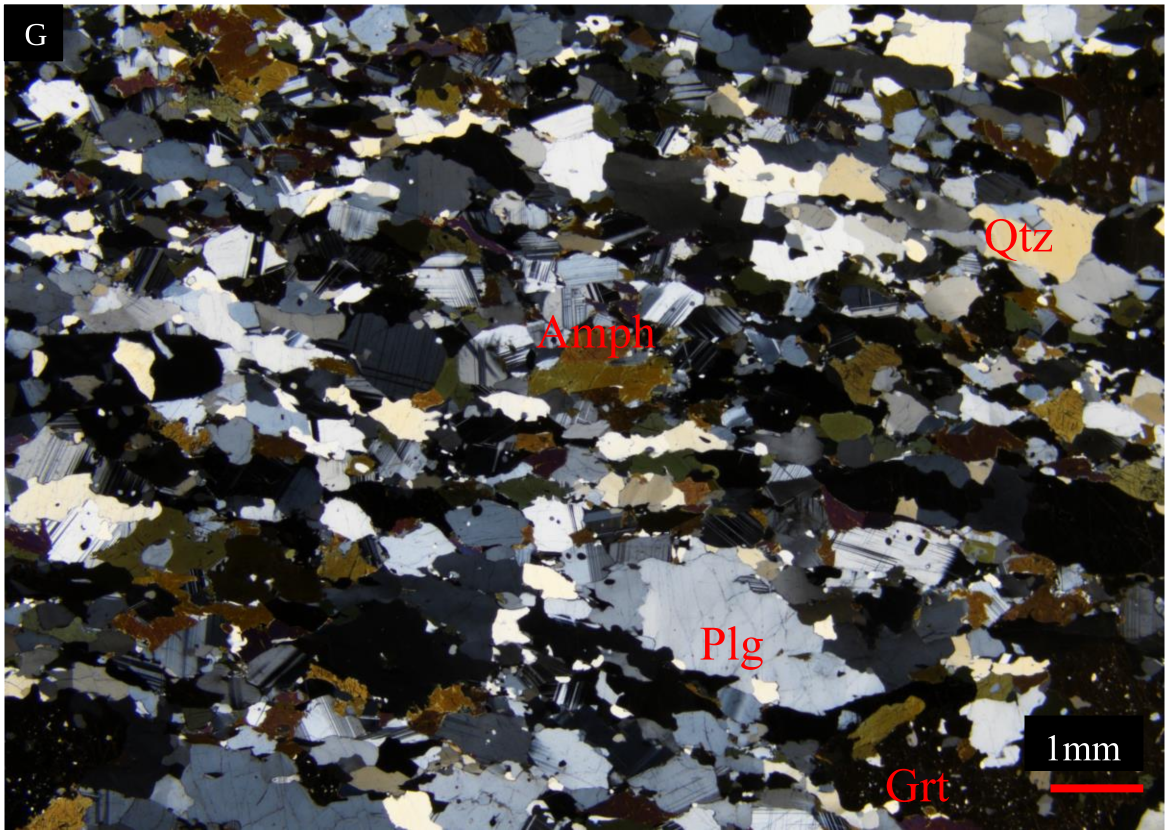

Figure 4.8

Variance of migmatized zones in the Dadeville Complex at locations 35, 40, and 48 near Chambers County Public Lake. (Quartz=Qtz, Biotite=Bt, Muscovite=Ms, Alkali feldspar=Alk, Plagioclase=Plg, Amphibole=Amph, Pyroxene=Px, Kyanite=Ky, Sillimanite=Sill, Chlorite=Chl, Garnet=Gt) **A.)** Migmatitic pod at location 35. **B.)** Boudinaged dilation structure at location 35. **C.)** Isoclinal folds at location 40. **D.)** Pavement outcrop at location 48. **E.)** Stromatic structures at location 48. **F.)** Escape structures at location 48. **G.)** Thin section from sample DCC-CB-27 at location 48.

The area within the Cusseta quadrangle where migmatization is highly pronounced is the west-central area around Chambers County Public Lake. A varying degree of migmatization is found within this area, from outcrops that contain small migmatized pods and boudinaged leucosomes containing feldspar and quartz (Loc. 35), sections with numerous isoclinally folded leucosomes (Loc. 38 and 40), and an extensive migmatized pavement outcrop with melt escape structures present (Loc 48) (Fig. 4.8 C-E). Other migmatized zones (Loc. 15 & 68) are found within the Cusseta quadrangle showing similar structures like those found near Chambers County Public Lake. These migmatitic zones found throughout the Dadeville Complex are classified as dilation structured and stromatic structured metatexite migmatites.

The pavement outcrop at location 48 approaches a diatexite morphology but can still be classified as mostly a metatexite. This area and location 72 (Fig. 4.9), just outside of the entrance to Chambers County Public Lake, show well developed stromatic metatexite structures and isoclinal folds with a large portion of the leucosomes gathering at the axial hinge with leucosomatic veins running parallel to the fold hinge. Numerous epidotized sections are present at location 72, this being the only migmatized outcrop within the quadrangle where epidote can be found in this great of quantity. This location and its immediate surrounding area indicate they experienced the most intense strain and melting within the quadrangle. The frequency and intensity of migmatites within the quadrangle decreases greatly when moving away from this area.

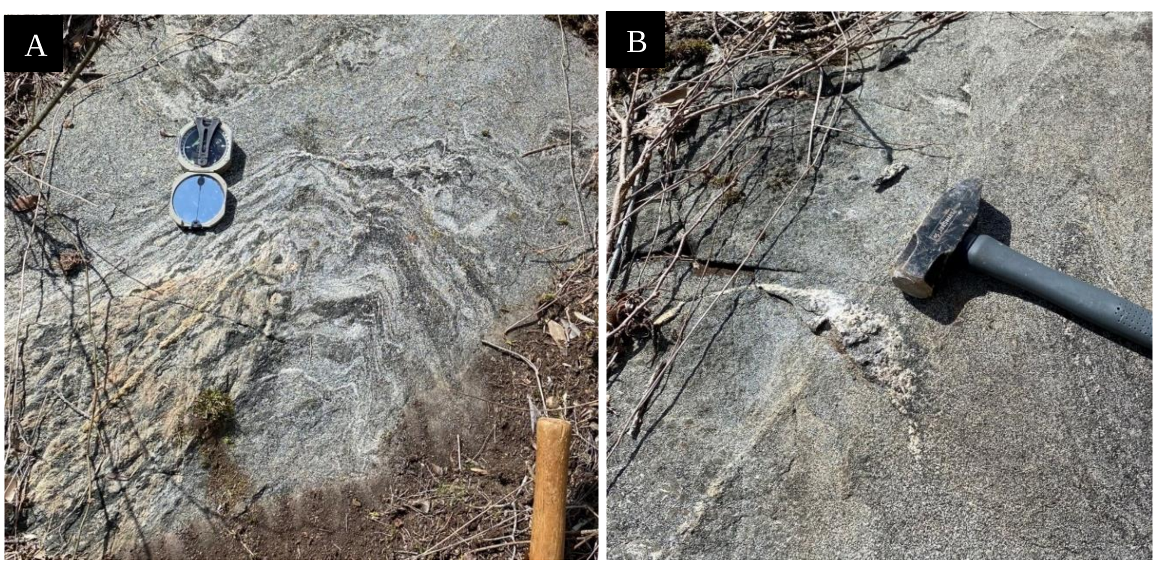

Figure 4.9

Highly stromatic metatexite migmatite section found in the Dadeville Complex at location 72 near the entrance of Chambers County Public Lake. **A.)** Stromatic structure with a leucosomatic vein running along the axial hinge of the fold. **B.)** Leucosomatic pod showing isoclinal folding with vein running through axial hinge. **C.)** Epidotized zone below an amphibolite section.

The leucosomatic veins and leucosomes consisting of plagioclase feldspar and quartz define the foliation plane at these outcrops. There are other examples where leucosomes crosscut the main foliation, especially when they are of larger volume. Leucosome width throughout these locations ranges from a few cm to tens of cm.

The migmatized zone (Loc. 15) (Fig. 4.2 D) found in the Loachapoka Schist of the Opelika Complex shows a similar first and second degree migmatitic morphology to that of the Dadeville Complex migmatites, a stromatic structured metatexite, but instead with a highly micaceous metapelitic paleosome.

4.4 Geologic Mapping of the Cusseta Quadrangle

Strike measurements plotted from mineral foliations within both the Dadeville Complex and Opelika Complex have a dominant orientation parallel to the Stonewall Line of NE and SW. Refer to Appendix A Table A.2 for associated geologic field mapping measurement data. The dip direction within the Dadeville Complex, close to the Stonewall Line within the SE quadrant of the quadrangle, is primarily to the NW. Moving further away from the Stonewall Line, within the Dadeville Complex, the overall dip direction changes to a dominant SE directed pattern throughout the rest of the quadrangle (Fig. 4.10).

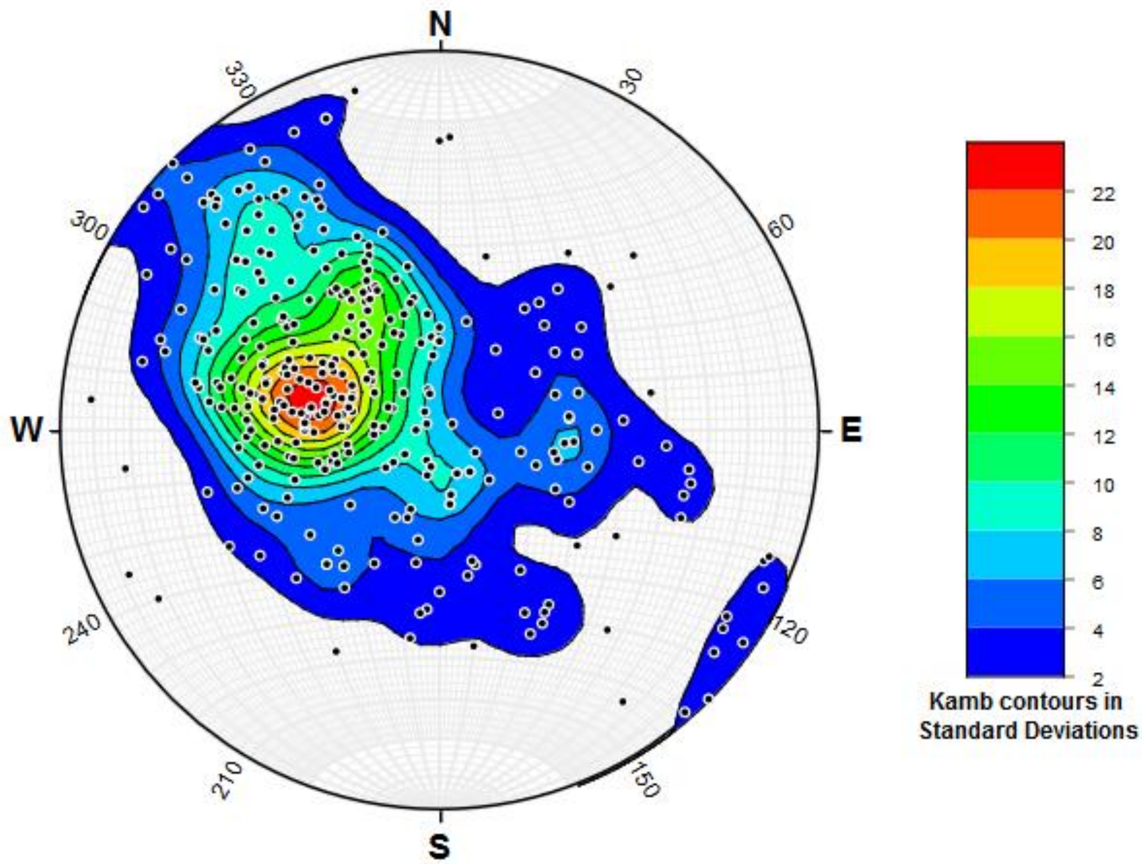

Figure 4.10

Kamb contoured poles from planes of metamorphic mineral foliations within the Dadeville Complex. Plotted using Stereonet (Allmendinger et al., 2012; Cardozo and Allmendinger, 2013).

This pattern would suggest a synformal feature is present, as initially suggested by Bentley and Neathery (1970) which they called the "Cusseta Synform". Strike measurements within the central section from the northern to the southern boundary (Loc. 4, 7-12, 18&19, 33, 56-63, 70) of the quadrangle alternate between NW to SE with a NE dip direction and NE to SW with a SE dip direction, indicating the likely presence of two sets of folds. The hinge line for the synformal feature trends to the NE (Fig. 4.11) at 032 and plunges shallowly at 04. The western section from the northern to the southern boundary (Loc. 21-32, 35-50, 52-55, 72) of the quad shows a similar trend for the hinge line, but slightly more easterly directed as compared to the central section, which trends more NE (Fig. 4.12) 070 and a steeper plunge of 24.

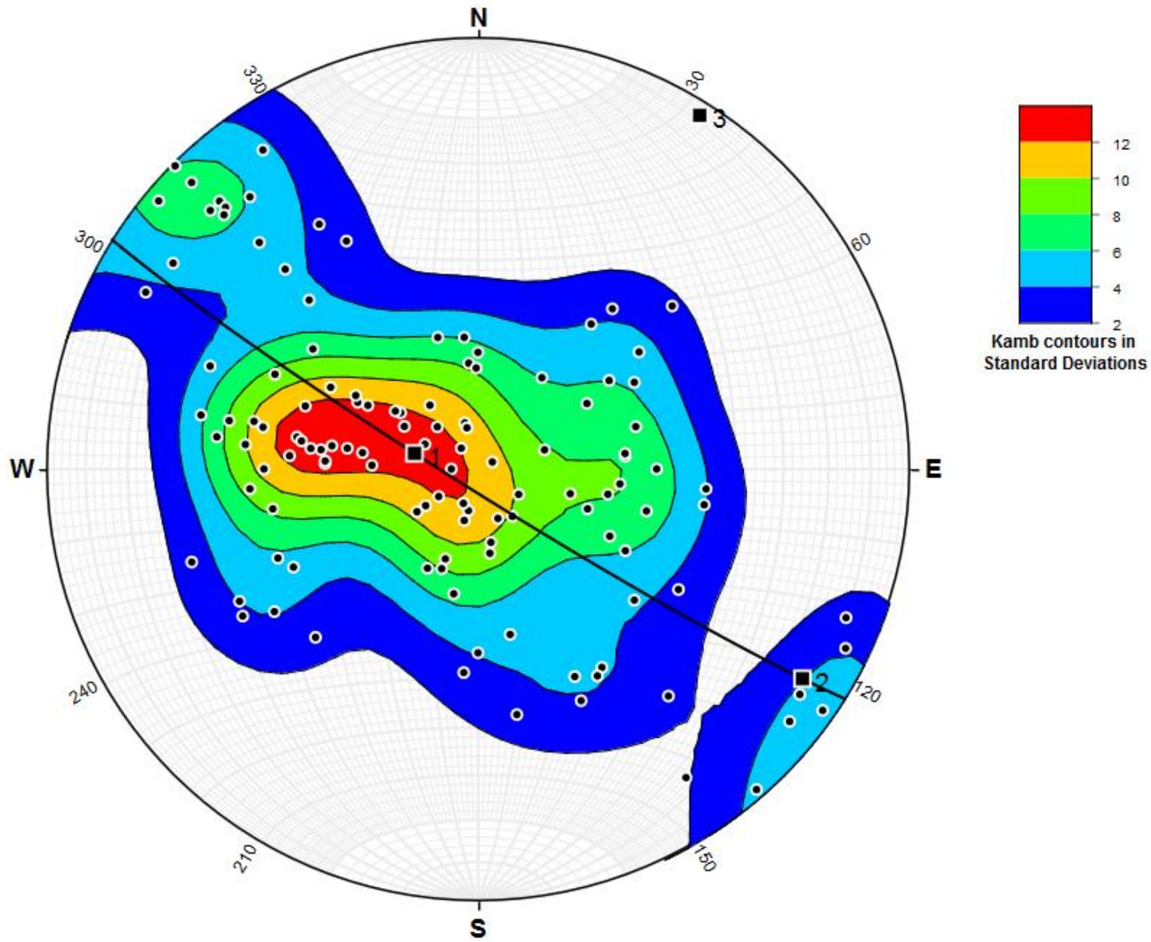

Figure 4.11

Kamb contoured poles and cylindrical best fit from planes of metamorphic mineral foliations within the Dadeville Complex of the central region. A cylindrical best fit is shown (black line), with an orientation of 04→032 (box 3). Plotted using Stereonet (Allmendinger et al., 2012; Cardozo and Allmendinger, 2013).

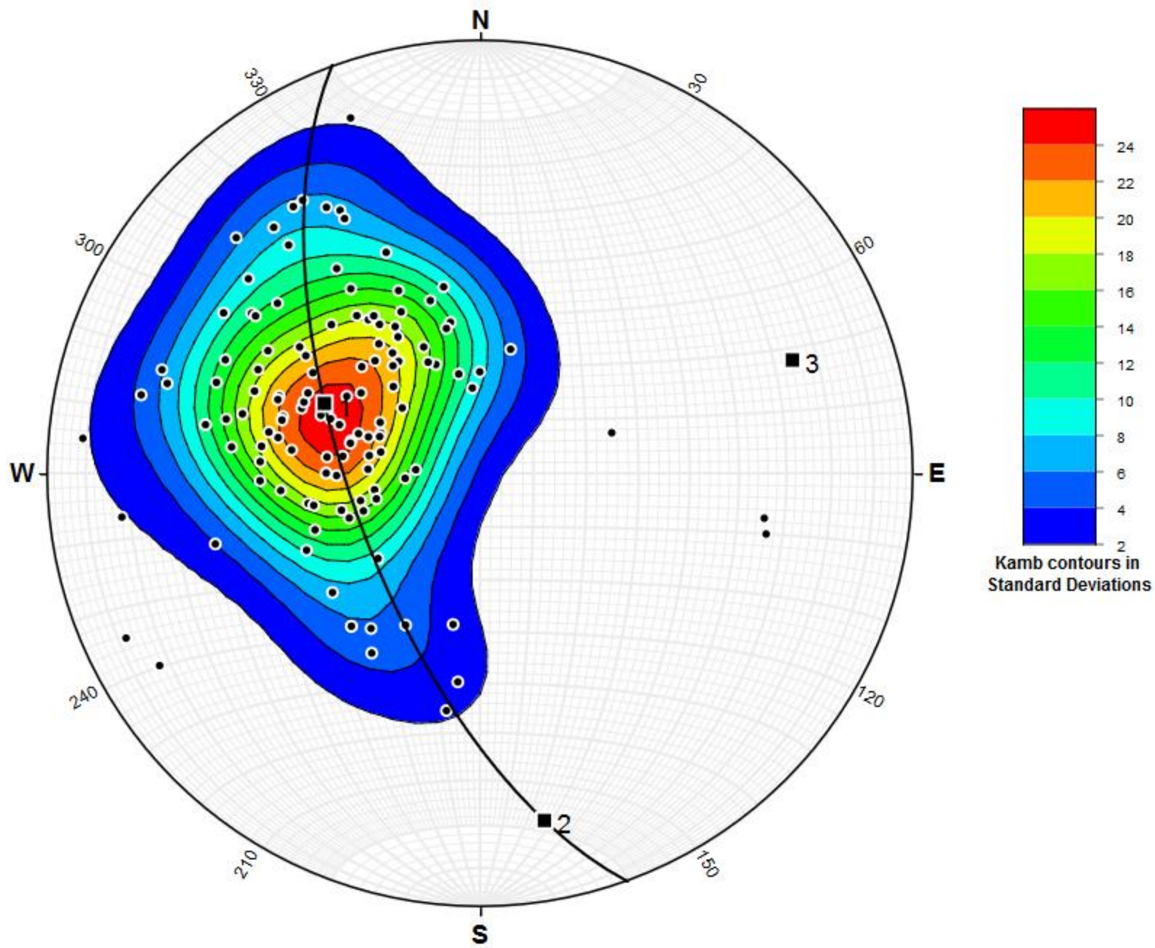

Figure 4.12

Kamb contoured poles and cylindrical best fit from planes of metamorphic mineral foliations within the Dadeville Complex of the western region. A cylindrical best fit is shown (black line), with an orientation of 24→070 (box 3). Plotted using Stereonet (Allmendinger et al., 2012; Cardozo and Allmendinger, 2013).

Similar to the Dadeville Complex, strike measurements from the Opelika Complex are oriented NE to SW. Unlike the Dadeville Complex, the overall dip direction for most the Opelika Complex shows a dominant NW directed orientation within the Loachapoka Schist, except for the Farmville Metagranite, where dip direction is to the SE (Fig 4.13). Outliers of poles found in Figure 4.13 in the NW of the stereonet are from the Farmville Metagranite showing the different dip direction in comparison to the Loachapoka Schist.

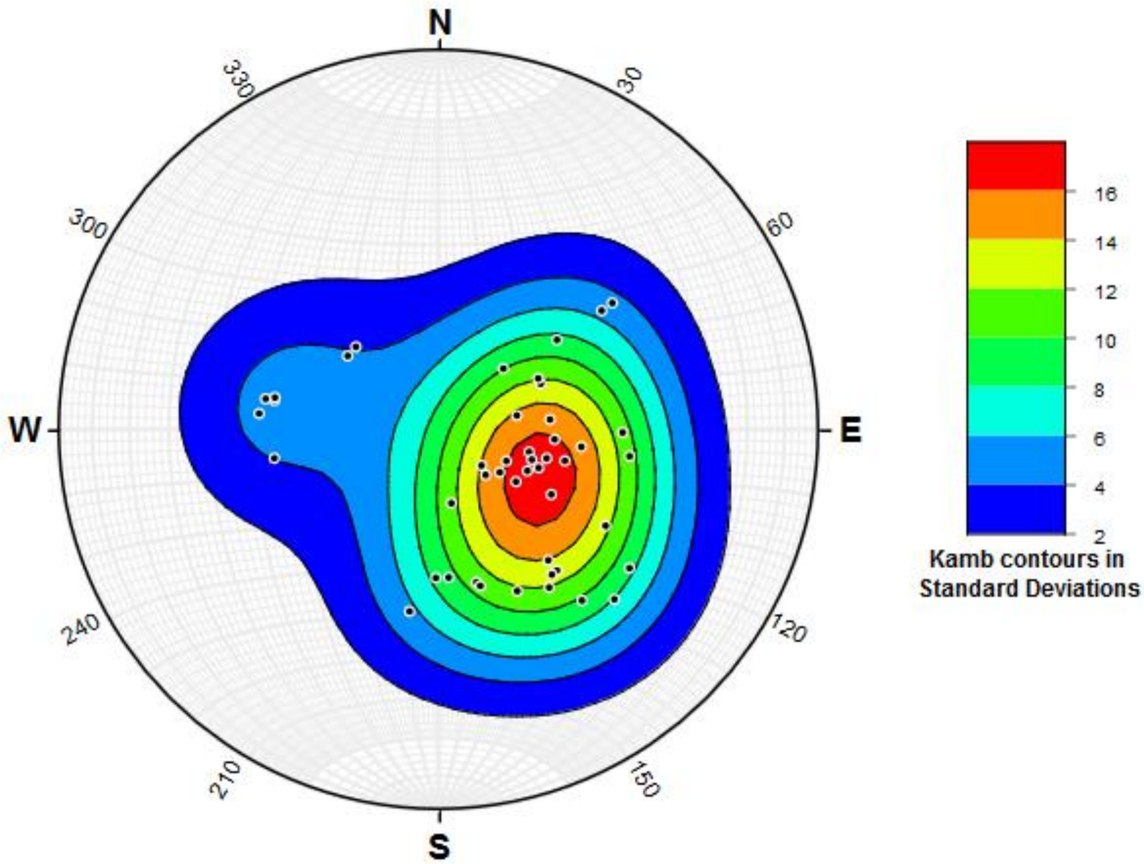

Figure 4.13

Kamb contoured poles from metamorphic mineral foliations within the Opelika Complex. Plotted using Stereonet (Allmendinger et al., 2012; Cardozo and Allmendinger, 2013).

Mineral lineations within the Cusseta quadrangle show trends primarily directed in an E-NE direction. Similar to how dip direction differed in the SE quadrant; both the Dadeville Complex and Opelika Complex have lineations within the SE quadrant that plunge NW and SE (Fig. 4.14 & 4.16). Lineations in the rest of the quadrangle are similar to the dip direction, primarily to the east.

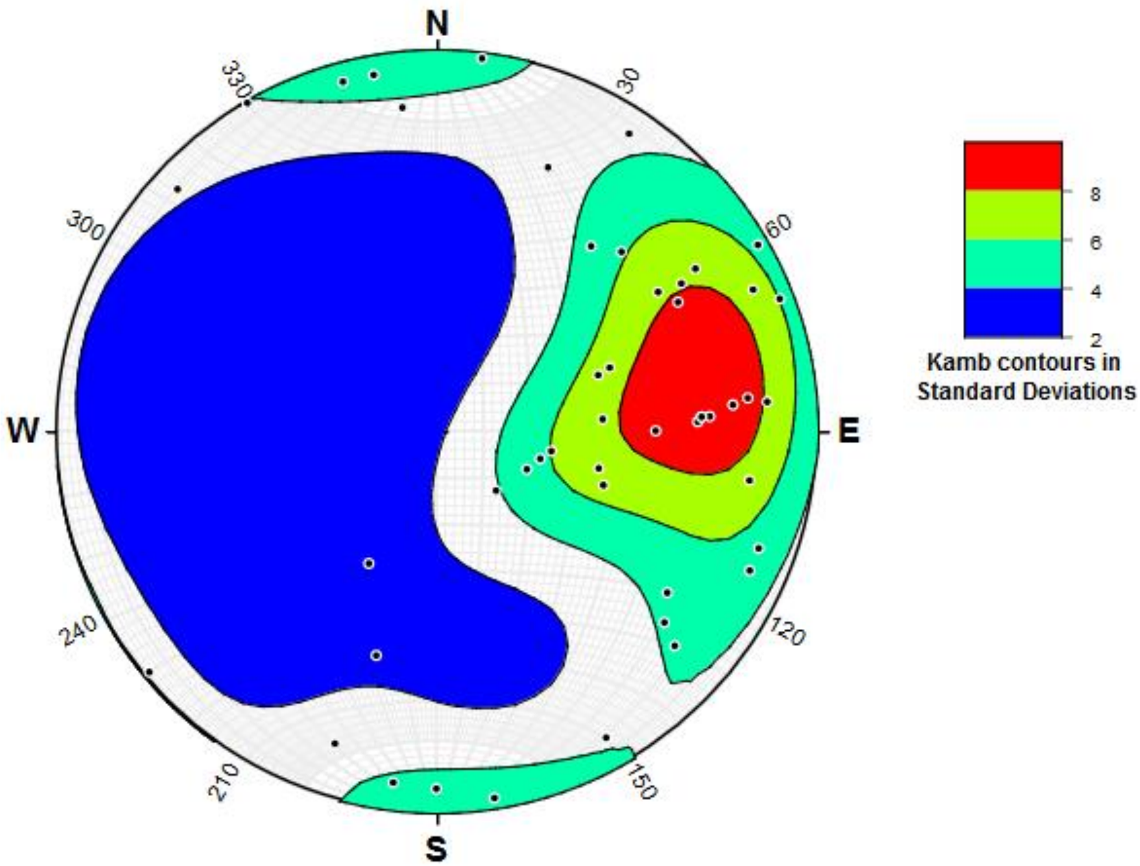

Figure 4.14

Kamb contoured metamorphic mineral lineations within the Dadeville Complex. Plotted using Stereonet (Allmendinger et al., 2012; Cardozo and Allmendinger, 2013).

Shallowly plunging lineations are found along the margin (Stonewall Line) of the Dadeville Complex and Opelika Complex and in the northern extent of the Cusseta quadrangle. The steepest plunging lineations are found in the central to southwest section of the Cusseta quadrangle, from north of location 21 to south of location 40 and as far east as location 33, trending east.

Lineations close to the Stonewall Line in the Dadeville Complex trend primarily to the N-NW and are gently plunging. The rest of the lineations plotted throughout the Dadeville Complex have a dominant east directed trend and are shallow plunging. Figure

4.15 shows the comparison of dip vs plunge for a given foliation-lineation pair with shear sense found within the Dadeville Complex throughout the quadrangle. The one-to-one slope as illustrated by the blue line and defined by the points close to the line represent dip-slip shear sense, while points within the middle indicate oblique slip, and points below a ten-degree plunge indicate strike-slip motion. Locations 19, 21, 25, 31, 33, 41, 62, and 63 all plot close to the line indicating a dominant dip-slip shear motion.

Geographic variability of these locations confine the dip-slip shear from the SW to the central NW section of the Cusseta quadrangle around Chambers County Public Lake. Locations 32, 36, 42, 55, and 68 show oblique-slip and all occur in the NW section of the quadrangle except for location 68, which occurs in the SE section of the quad. Locations 48, 49, 58, and 69 show strike-slip and all occur in the central to NW section of the quad except for location 69 in the SE section of the quad near Cusseta.

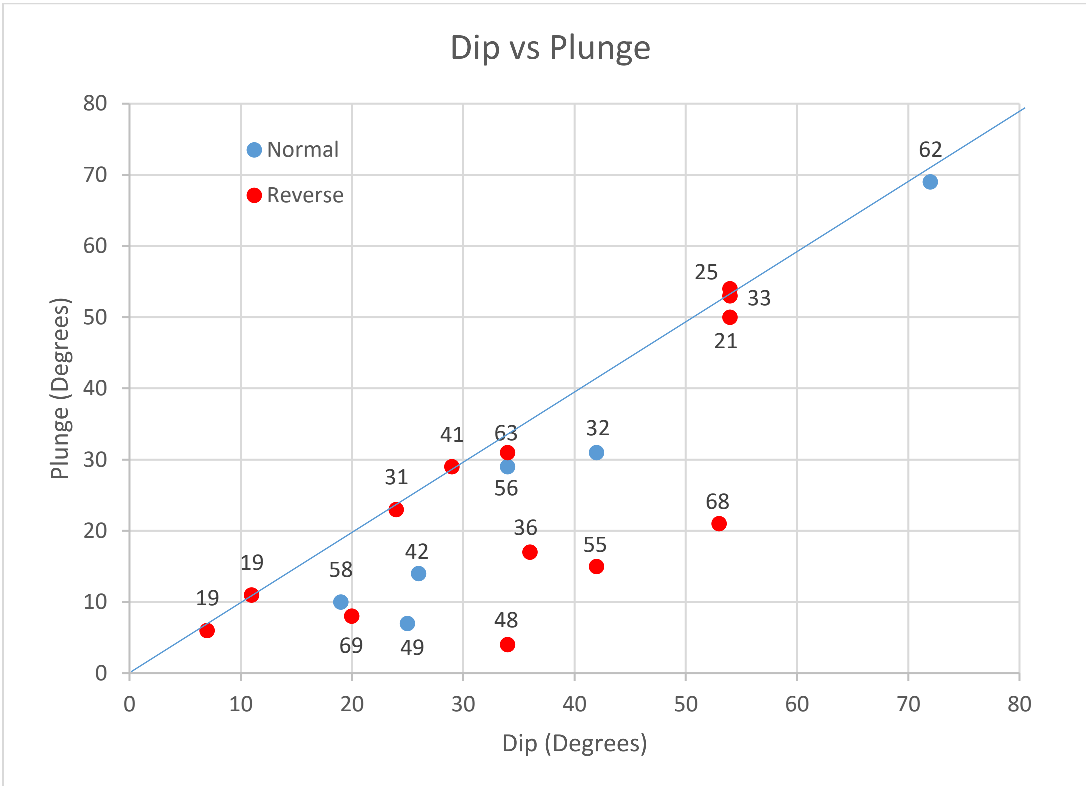

Figure 4.15

Plot showing dip vs plunge with associated shear sense within the Dadeville Complex. Points are labeled with associated locations.

Lineations from the Opelika Complex are shallowly plunging and trend primarily to the NW and SE. Four lineations are plotted within the Loachapoka Schist. Two of them, which are inside the boundary of the Cusseta quadrangle, trend to the NW and SE. The other two, one being outside the southern boundary (Loc. 3) of the quadrangle, trends to the NE, the other located to the east of the boundary (Loc. 2), trends to the NW. The lineations in the Farmville Metagranite trend SW and plunge shallowly.

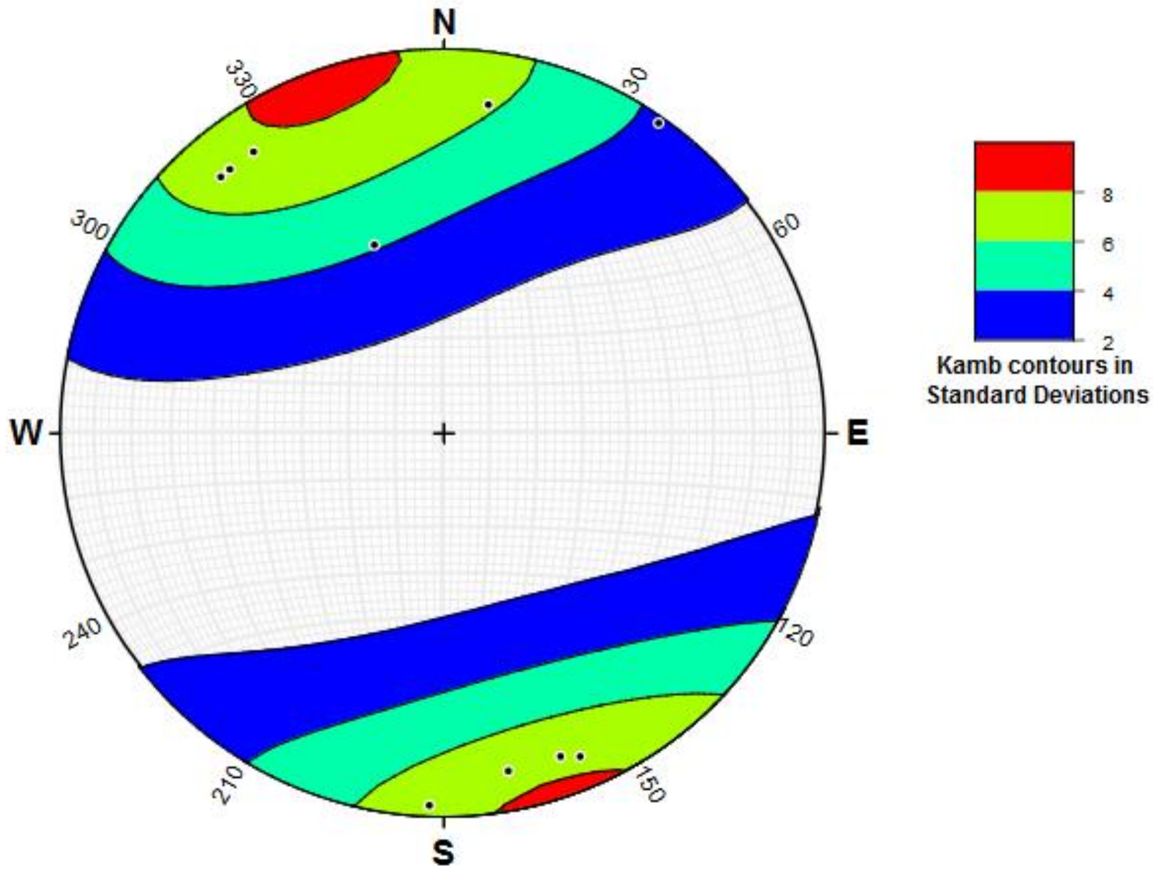

Figure 4.16

Kamb contoured metamorphic mineral lineations within the Opelika Complex. Plotted using Stereonet (Allmendinger et al., 2012; Cardozo and Allmendinger, 2013).

4.5 Shear Kinematics of the Cusseta Quadrangle

Twenty-two shear sense indicators were determined within the Cusseta quadrangle, and the twenty-third outside the boundary at location 2. Of the twenty-two, fourteen are reverse shear sense with the remaining eight being normal shear. Thirteen of the fourteen reverse shear senses are plotted in the Dadeville Complex with the other in the Opelika Complex. Seven show dip-slip, three show oblique-slip, and two show strike-slip within the Dadeville Complex. Seven of the eight normal shear senses are plotted in the Dadeville Complex (Fig. 4.17), with the other in the Opelika Complex. One shows dip-slip, three show oblique-slip, two show strike-slip within the Dadeville Complex and one could not be determined. No comparisons in slip style were determined for the Opelika Complex.

The dominant motion of shear sense indicators within the Dadeville Complex shows a top-up, reverse, NW directed shear with the RCA comprising most of the reverse shear sense indicators, with some normal shear sense also present. The Waverly Gneiss has mostly normal, top-down, E-SE directed sense of shear with some reverse shear present throughout. Location 55, the only outcrop documented to be the Agricola Schist, shows an oblique-slip reverse shear sense. Figure 4.18 shows the comparison of plunge vs shear sense found within the Dadeville Complex throughout the quadrangle on a stereonet. The overlap of both normal and reverse shear sense does not seem to indicate any easily distinguishable pattern in the Dadeville Complex other than that a dip-slip reverse shear sense seems to dominate the area.

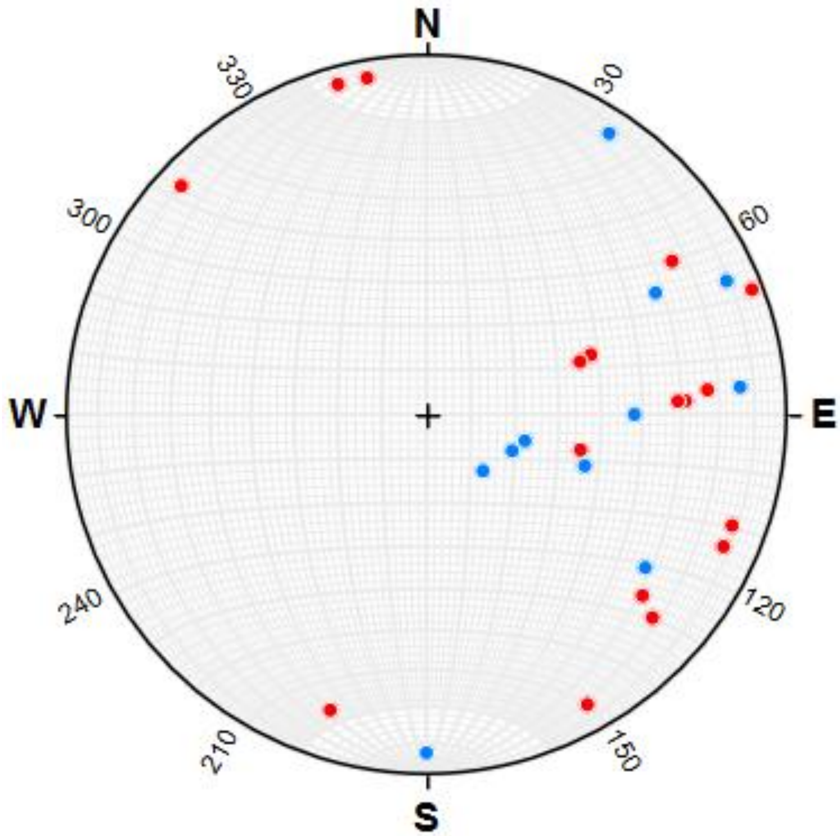

Figure 4.17

Shear sense indicators with all associated mineral lineations from outcrops within the Dadeville Complex (Blue=Normal; Red=Reverse). Plotted using Stereonet (Allmendinger et al., 2012; Cardozo and Allmendinger, 2013).

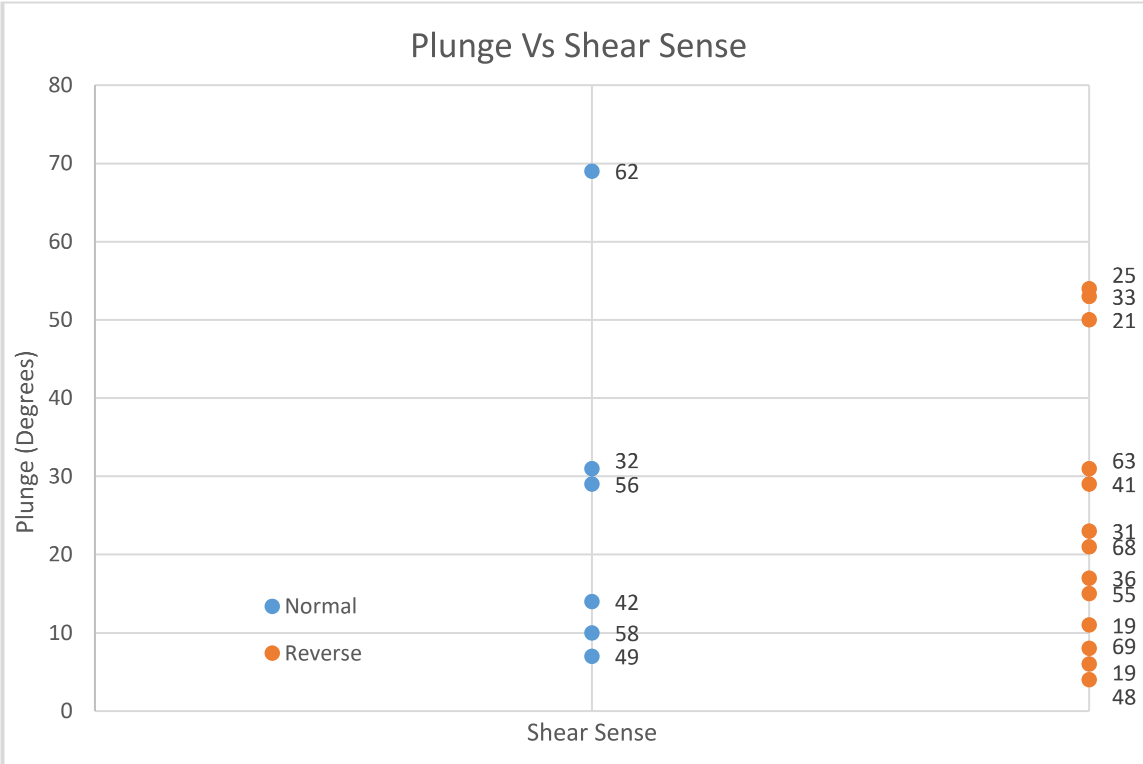

Figure 4.18

Plot showing plunge (degrees) vs shear sense within the Dadeville Complex. Points are labeled with associated outcrop locations.

The remaining two shear sense indicators are in the Opelika Complex (Fig. 4.19). One is in the Loachapoka Schist, and the other in the Farmville Metagranite. Shear sense indicators found in the Loachapoka Schist and Farmville Metagranite show both opposite shear type and direction. The sample collected from the Loachapoka Schist (Loc. 16), close to the Stonewall Line, shows a normal, top-down, SE directed shear sense. The sample collected from the Farmville Metagranite (Loc. 73) shows a reverse, top-up, north directed shear sense.

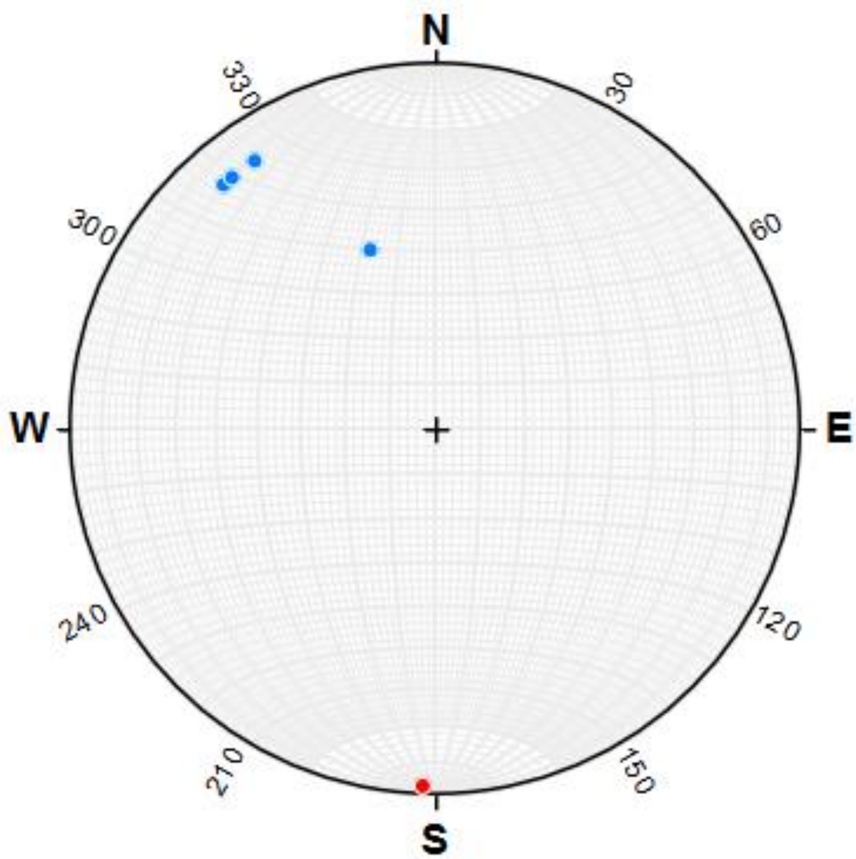

Figure 4.19

Shear sense indicators with all associated mineral lineations from outcrops within the Opelika Complex (Blue=Normal; Red=Reverse). Plotted using Stereonet (Allmendinger et al., 2012; Cardozo and Allmendinger, 2013).

CHAPTER V - DISCUSSION

In this section implications of geologic mapping, shear data, and fold geometry will be discussed and applied to the Dadeville and Opelika Complexes and the Stonewall Line observed in the Cusseta quadrangle. An interpretation in comparison and contrast to current models of translation of the Dadeville Complex will be made from mineral foliation, lineations, and shear kinematics collected from within the quadrangle. To form a model of this area, the following must be considered: 1) unit geometry in the Dadeville Complex, 2) most mineral lineations plunge to the east, 3) shear kinematics are mostly reverse, top to the NW, 4) timing of migmatization within the Dadeville Complex.

5.1 Fold Geometry within the Cusseta Quadrangle

The RCA and WG have outcrop patterns and foliations that indicate folding. Folding may become more complex during polydeformed systems from multiple orogenic events such as recorded in the Appalachian Mountains. Superposed fold geometry models have been described by Ramsay (1967) and Ramsay and Huber (1987), which they have defined as Types 0-3 (Fig. 5.1). Type 0 folds are folds that have undergone “redundant” superposition, which tightens and exaggerates the initial fold geometry. Type 1 folds have axial surfaces that intersect at a high angle. This Type 1 fold is also known as an “egg-carton” structure or a “dome-and-basin” pattern. Type 2 folds, also known as “boomerang” or “mushroom” folds are a result of an inclined axial surface superposed by folds with steeply dipping axial surfaces and hinge lines at high angles to each other. Type 3 folds, also known as “hook” folds, have recumbent folds that are refolded by an upright fold, which means the hinge lines are parallel, but the axial planes are perpendicular to each other.

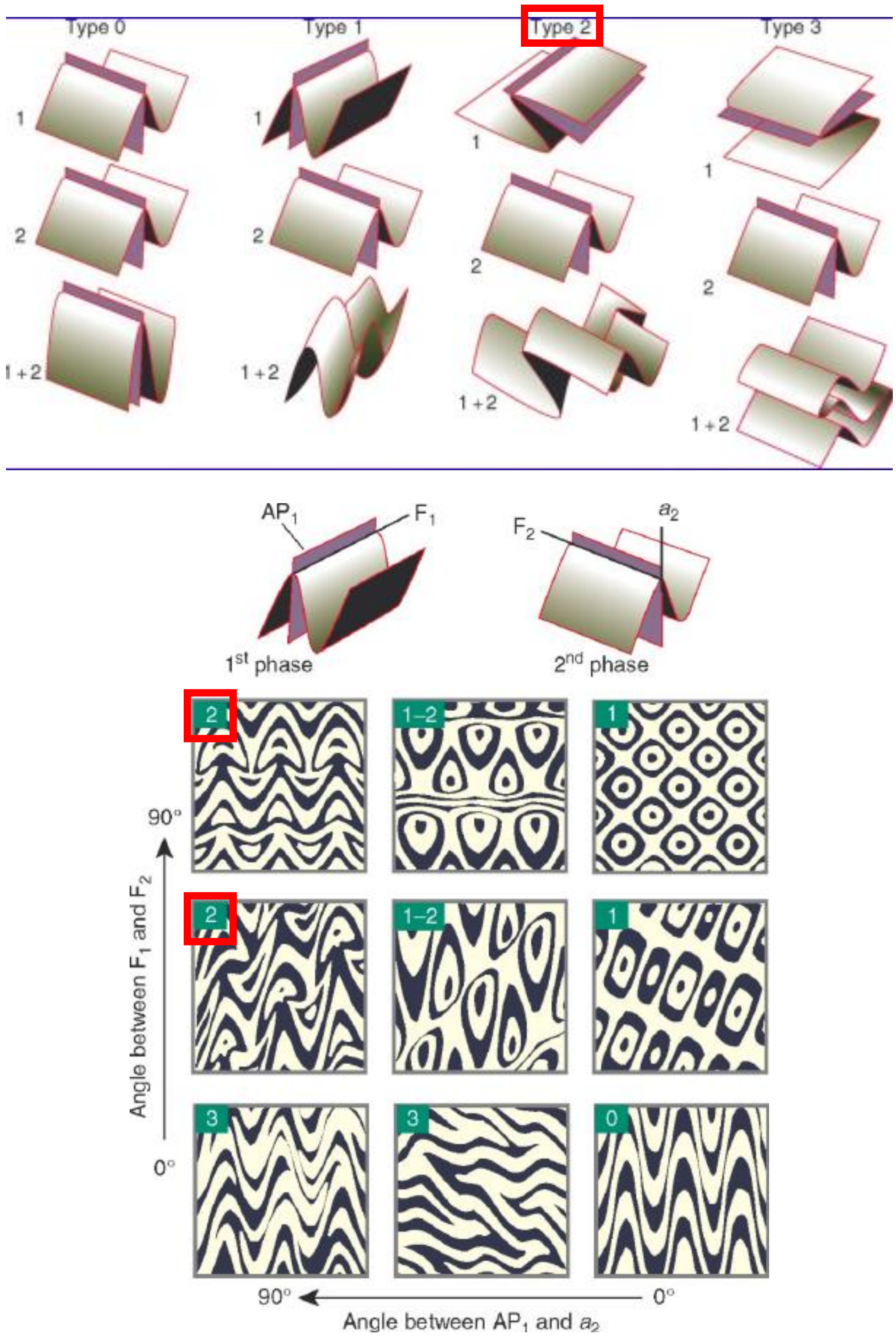

Figure 5.1

Fold interference patterns and implied map geometry of rock units (Modified from Thiessen and Means, 1980 & Ramsay and Huber, 1987). Type 2 fold pattern outlined in red with numbered rows indicating fold phases combining to make the fold type (F2).

It is evident, after interpreting geologic mapping data collected within the Cusseta quadrangle, that there are superposed folds present and a larger-scale synformal structure presently plunging NE known as the "Cusseta Synform" by Bentley and Neathery (1970). Repetitious patterns are found alternating between the RCA and Waverly Gneiss throughout the quadrangle in the Dadeville Complex. Foliation patterns define open to closed folds, however, many of these folding patterns are disharmonic and oppose each other. The localized sections of the Waverly Gneiss seem to indicate a mushroom surface expression based on foliation patterns, namely locations 18 and 19 and 57 and 58, with the RCA encapsulating unit banded between the Waverly Gneiss. This boomerang pattern is recognizable through geologic surface mapping geometry throughout the Dadeville Complex within the quadrangle and likely indicates a Type 2 superposed fold geometry.

Interpreting the Type 2-fold geometry and direction of fold vergence indicates that the shape of the mushroom pattern of the F2 hinge lines trending E-W. F1 folds have the opposite trending fold hinge, which trends N-S. This interpretation is not far off from what is presented in the Alabama state map within the Cusseta quadrangle (Osborne et al., 1988). The map shows banded RCA and Waverly Gneiss with two folds; one fold set on the western half of the quadrangle with a hinge line trending N-S and another fold set on the eastern half of the quadrangle with a hinge line trending E-W. The map presented here (Fig. 5.2) took these same patterns as the Alabama state map and interpreted them with models of superposed folding (e.g., Ramsay, 1967).

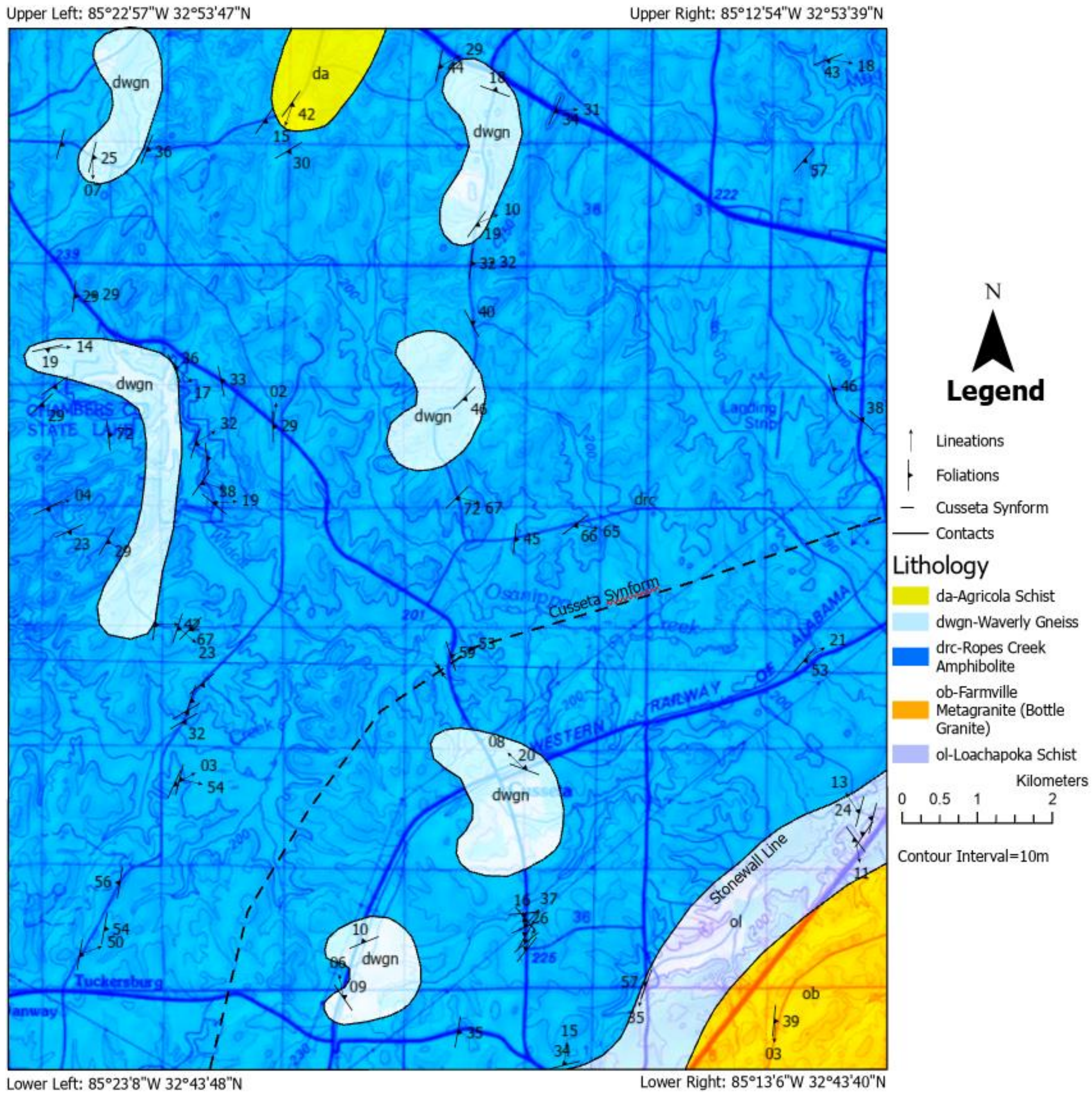

Figure 5.2

Geologic map of the 7.5' Cusseta Quadrangle illustrating structural data and lithologic contacts with newly interpreted superposed fold geometry created by ArcGIS Pro.

Given the orientation of F1 and F2, the simplest interpretation is that the shortening direction for F1 and F2 were perpendicular to each other, with F1 shortening axes-oriented E-W forming a reclined to recumbent fold geometry and F2 shortening axes-oriented N-S forming a mostly upright fold geometry. This indicates an almost 90°

change in orientation of the shortening axes between F1 and F2 in a relative short period of time.

Most mineral stretching lineations are defined by hornblende and/or plagioclase within the Cusseta quadrangle. The mineral lineation orientation is mostly plunging to the E, but there is some scatter with a subset plunging to the N and S. The mineral lineations are parallel to the interpreted trends of the F1 (N-S) and F2 (E-W) folds (Fig. 4.10), indicating both folding events occurred at higher temperature, in this case, peak metamorphic conditions at amphibolite grade. Mineral lineations that do not trend N-S or mainly E may have been scattered due to F2 folding. The map pattern of the Dadeville Complex within the Cusseta quadrangle suggests that the F2 folds which formed from a D2 event (Neoacadian) are the last significant overprint within the Dadeville Complex.

Topography also plays a role in interpreting the geographic spacing of units within the Cusseta quadrangle. Units within the Dadeville Complex, like the RCA and Waverly Gneiss, are found in locations that have higher elevation in comparison to the Agricola Schist. The Agricola Schist has been interpreted as the sedimentary cover of the Dadeville Complex, and therefore should be at higher elevation than the meta-igneous rocks (Tull et al., 2018). The interpreted fold geometry of Type 2 folds predicts that the structurally highest unit, in this case the Agricola Schist, would be in the trough of the Type 2 fold pattern, in this case the troughs have a N-S bearing. The fold troughs are also the locations of first and second order fluvial systems and paludal environments, which likely led to erosion of the Agricola Schist especially to the south towards the Coastal Plain, explaining why the fluvial systems formed in this area and why the Agricola Schist is only found in the northern part of the quadrangle, leaving only exposures of the underlying RCA and Waverly Gneiss.

The stream shapes within the quadrangle show a trellised to rectangular drainage pattern. These patterns indicate that lower order streams join the master stream at almost right angles and are heavily influenced and guided by the strike and dip of the surrounding rock units. The main tributary that runs through the Cusseta quadrangle draining east into the Chattahoochee River has lower order streams that run perpendicular to strike and parallel to the overall dip direction within the quadrangle.

There are some irregularities to the folding patterns, namely in the southern third and along the western edge of the quadrangle. In the southern third, the folding pattern within the RCA is closely spaced and tight, exemplified by locations 4-11, 21-23 and 26-29. These folds have similar orientations as the broader folds described above with locations 4-11 and 26-29 having hinges that trend E-NE and the folds at locations 21-23 having N-S trending hinges. These folds are closer to the Stonewall Line, so they may have been further tightened due to strain along the Stonewall Line.

Along the western margin of the quadrangle is the location of the majority of the migmatites. The migmatites would have been much weaker compared to the unmelted RCA, making the migmatites more likely to partition strain and even dome due to buoyancy contrasts with surrounding rocks. This may have led to the disrupting of folding patterns and doming.

5.2 Models of Terrane Emplacement

Most authors agree that the Dadeville Complex is a structurally synformal, allochthonous Taconian arc and back-arc system (Sears et al., 1981; Neilson and Stow, 1984; Steltenpohl et al., 1990; Steltenpohl and Kunk, 1993; Farris et al., 2017; Tull et al., 2018; Ma et al., 2019). However, the movement of the Dadeville Complex from its origin to current emplacement is less agreed upon. As stated previously, reports by several authors suggest that the Dadeville Complex was moved by means of either orogen parallel translation (Steltenpohl, 1988; Ma et al., 2019), klippe kinematics along the Brevard Fault Zone, Stonewall Line, and to some extent the Towaliga Fault Zones (Sears et al., 1981, Tull and Holm, 2005; Farris et al., 2017; Tull et al., 2018), and/or crustal/channel flow (Merschat et al., 2005; Hatcher and Merschat, 2006).

Merschat et al. (2005) and Hatcher and Merschat (2006) indicate crustal flow for the Tugaloo Terrane in South Carolina and Georgia. The Tugaloo Terrane is part of the IP and of similar lithology of the Dadeville Complex. This similarity may indicate that the Dadeville Complex experienced similar internal strain through channel flow as it was pinned against Laurentian basement and the Carolina superterrane during accretion.

5.2.1 Channel Flow

If channel flow is to be expected throughout the Dadeville Complex, as suggested by Merschat et al. (2005) and Merschat and Hatcher, (2006) in the central Appalachian Mountains, along strike SW directed shear kinematics of micro to regional scale sheath folds should be evident throughout the Dadeville Complex and IP. Less deformation and shear should be present within the Opelika Complex as compared to the Dadeville Complex; this reasoning is that the Dadeville Complex is an allochthonous terrain transposed a significant distance, and the Opelika Complex is not. Strain would increase towards the middle of the Dadeville Complex, as the center of the orogenic channel would have the highest velocities, and the borders of the complex would be the lowest.

Mineral lineations for the Dadeville Complex would be expected to flow perpendicular to the Stonewall Line (NW), sometimes even NE, before curving SW indicating flow parallel to the Stonewall Line. The base of the channel should record top-to-the-SW shear sense and the top should record top-to-the-NE shear sense.

Very few SW directed shear kinematics were found within the Cusseta quadrangle and no evidence of sheath folds, at microscopic to macroscopic scale nor NE directed shear towards the top of the quad was found in the Cusseta quadrangle. Mineral lineations and foliations collected throughout the quadrangle indicate strike for foliations and trend for lineations are primarily parallel (E-NE) to the Stonewall Line. A N-NW trend of lineations (Loc. 3-5, 10, and 19) is perpendicular to the Stonewall Line, suggesting that from a mineral lineation and foliation perspective, channel flow is plausible, but more evidence supporting shear kinematics and evidence of sheath folds must be found to fully support it. Alternatively, superposition of folding could have overprinted the predicted pattern of foliations and lineations for channel flow. However, since most lineations are defined by plagioclase and hornblende indicating they formed during peak metamorphism, it is more likely some other process was more dominant within this area.

5.2.2 Klippe Kinematics

Sears et al. (1981), Tull and Holm, (2005), Farris et al. (2017), and Tull et al. (2018), suggested that the Dadeville Complex likely formed in a supra-subduction environment as part of an arc/back-arc assemblage on Laurentian lithosphere with evident klippe thrust sheets, requiring B-type subduction (continental upper plate), rather than the A-type subduction (oceanic upper plate). Sears et al. (1981) suggested that the IP was displaced at least 185 km in a northwestern direction (2-D shortening) from its original formation location and was at least 25km thick. Because of the thickness and the presence of well-developed shear zones (i.e., Brevard Zone) workers (e.g., Sears et al., 1981) have proposed that most of the IP's core was strained very little. Lineations that are perpendicular to the fault/shear zones and parallel to dip (Stonewall Line in this case), should be present along with top to the W-NW reverse kinematics. This would indicate the thrust component of the klippe feature is present at the basal thrust (Stonewall Line) as is suggested by Sears et al. (1981), Farris et al. (2017), and Tull et al. (2018).

Close to the Stonewall Line, lineations associated with F1 within the Dadeville Complex trend oblique to parallel along the margin, which is also parallel to dip direction (N-NW). Farther away from the Stonewall Line into the Dadeville Complex, the dip direction of foliations is primarily SE and lineations trend oblique to the margin (E to slightly NE), but perpendicular to dip. Folding within the RCA near the Stonewall Line is tighter and has a smaller wavelength compared to the northern part of the quadrangle. Into the Opelika Complex, dip direction of foliations is primarily to the NW. Shear sense is mostly reverse to the NW throughout most of the quadrangle but is not found close to the Stonewall Line. This model is justified close to and along the Stonewall Line within the Cusseta quadrangle through lineation direction and tightening of folds. However, shear direction throughout the quadrangle and extensive, penetrative strain throughout the quadrangle does not match these predictions of NW shortening, but other directions of shortening, namely E-W for F1 and N-S for F2, would form by similar mechanisms.

5.2.3 Orogen-Parallel Translation

If orogen parallel translation from the Tennessee embayment as suggested by Ma et al. (2019) is the primary mechanism of movement of the Dadeville Complex and IP, dextral, strike-slip, shear kinematics will be present along the northern and southern contacts of the Dadeville Complex (Brevard FZ and Stonewall Line) with little shear present within the central core of the complex. This mechanism of dextral translation has been suggested by many including, but not limited to, Steltenpohl (1988), Snoke and Mosher (1989), Snoke and Frost (1990), Goldberg and Steltenpohl (1990), and Ma et al. (2019).

Steltenpohl (1988) stated that dextral shear during the Alleghanian orogeny affected rocks as far as 5 km into the Opelika Complex of the IP north of the Towaliga FZ. Steltenpohl (1988) also stated that button schists within the IP contain pervasive unidirectional (SE) shear bands and sigmoidal quartz-feldspar composites. The kinematic analysis within the Steltenpohl (1988) report is consistent with other reports, indicating the last motion on the fault is dextral and normal in the Towaliga FZ (IP and Pine Mountain Window boundary), which should be evident within the Opelika Complex, meaning dextral shear bands should be present running parallel to the slip vector (Stonewall Line).

Ma et al. (2019), stated that because the Dadeville Complex (RCA & Agricola Schist) was metamorphosed at upper amphibolite to lower granulite facies conditions, with P-T estimates of up to 700 to 800 °C and 8 to 10 kbar, ductile shear zones within the Dadeville Complex should exhibit sub-horizontal, northeast-trending stretching lineations that postdate the peak metamorphism because of Alleghanian aged greenschist-grade overprinting relationships of mineral assemblages. This would suggest the Dadeville Complex was likely transported at mid-crustal levels along the Brevard FZ, next to the adjacent Eastern Blue Ridge from the Tennessee embayment to the Alabama promontory due to the dextral transpression associated with the Neoacadian orogeny. If orogen-parallel translation is expected to be recorded within the Cusseta quadrangle, dextral strike-slip shear indicators should be most evident near the Stonewall Line with lineations trending NE and dip vectors striking NE, with right-lateral kinematics, and decreasing strain away from the Stonewall Line.

Sub-horizontal, E-NE, trending lineations are present throughout most of the Dadeville Complex; however, no significant greenschist grade mineral assemblage overprint (except chlorite within the Agricola Schist) or overprint of S-C fabrics were seen in thin section nor is mostly dextral strike-slip evidence present. The migmatized zones within the RCA seem to follow similar strike/dip and lineation patterns in most of the quadrangle, indicating that the migmatites formed during peak metamorphism during the Acadian-Neoacadian orogeny. Some outcrops exhibit a mild strike-slip shear sense, mostly left lateral, but the majority within the Dadeville Complex show reverse sense with top-up directed NW, and outcrops within the Opelika Complex showing no evidence of strike-slip motion. The lack of overprinting of greenschist grade assemblages and fabrics found within the Cusseta quadrangle indicate that this area was not significantly affected by the Alleghanian orogeny.

The Opelika Complex did show a significant increase in grain size (Fig. 4.2F) approaching the Stonewall Line with an assemblage indicating middle-upper amphibolite grade metamorphism. It is likely this increase in grain size was syn-peak metamorphism during early to late Neoacadian orogeny, where prograde metamorphism of amphibolite grade occurred during the Devonian Period. Continuation of similarly striking foliations within the Dadeville Complex are present close to and at the Stonewall Line and within the Loachapoka Schist, suggesting that superposed F1 and F2 folds present must have occurred during the Acadian-Neoacadian orogeny.

5.2.4 Suggested Model

None of the three suggested models (channel flow, klippe kinematics, or orogen-parallel translation) completely show a clear indication of how the Dadeville Complex was emplaced to its current location or can explain the superposed folding pattern. This could be from a lack of strong evidence within the Cusseta quadrangle fully supporting these models given the fact that this is too small of a study area to base a means of movement for an entire complex, or that on smaller scale observations indicate that the deformation of the Dadeville Complex was heterogeneous.

A combination of the previously published models and data gathered from the Cusseta quadrangle appear to suggest how the Dadeville Complex was emplaced. Mineral foliation and lineation data support the argument for channel flow to an extent, but there is a considerable lack of shear compatibility and a lack of sheath folds. For klippe kinematics, foliations and lineations align with this model close to the Stonewall Line, and the overall trend of shear direction throughout the quadrangle aligns as well. East to NE trending mineral lineations also somewhat support orogen parallel translation, but there is a considerable lack of suggested strike-slip shear sense indicators that would be from translation during the Acadian orogeny. Greenschist facies mineral assemblage overprint from the Alleghanian orogeny is also not as pervasive throughout the quadrangle.

The Stonewall Line within the Cusseta quadrangle was an inferred boundary between outcrops of the Loachapoka Schist and RCA and therefore lacks evidence to help identify the margin's likely cause. A model based on the results presented here would suggest that the Stonewall Line is a zone of weak shearing and zone of movement for the Dadeville Complex emplacement. How the Dadeville Complex was emplaced shows aspects of models with mostly klippe-thrust movement along the basal contact (Stonewall Line) where it was transposed to its current emplacement likely through orogen-parallel translation during the Acadian orogeny.

It is this author's suggestion that that the Dadeville Complex was emplaced to its current location through tectonic processes creating F1 folds that occurred during peak metamorphism within the IP during the Acadian orogeny forming the recumbent geometry indicating these folds to be highly strained where lineations trend N-S with shortening occurring E-W and fold vergence to the west. This indicates that F1 folds likely occurred during the early Acadian orogeny when the Rheic Ocean (Cat Square terrane) was subducting under the approaching Carolina superterrane while the IP was also accreting NW to the Laurentian margin (Huebner et al., 2017). F2 folds occurred and overprinted F1 folds during the Neoacadian orogeny as the Carolina superterrane overrode the Cat Square terrane and IP when accreting to the Laurentian margin. This caused crustal thickening and anatexis leading to the formation and emplacement of the migmatites within the IP.

The collision of the Carolina superterrane was oblique during the Neoacadian orogeny and eventual closing of the Rheic basin from the NE to SW starting around New York. This oblique collision could have resulted in different shortening directions compared to the Acadian orogeny at this latitude and could explain the sharp contrast in hinge orientation and interpreted shortening direction between F1 and F2 in a geologically short period of time. During one of these collisions, the Dadeville Complex and Opelika Complex must have been juxtaposed along the Stonewall Line. Given the rheologic contrast between the two complexes, the Stonewall Line likely preferentially partitioned strain, however, given the results here, the Stonewall Line acted mostly as a suture.

CHAPTER VI - CONCLUSION

After careful study, previously proposed models for the emplacement for the Dadeville Complex are not fully supported in the Cusseta 7.5' minute quadrangle and instead a protracted, polydeformational event ranging from the Taconic to the Neoacadian orogeny is favored. Evidence indicates that foliations strike NE to SW and primarily dip SE with mineral lineations within the quadrangle gently plunging slightly E-NE and primarily record reverse NW directed shear kinematics. F1 (Acadian) was likely a reclined to recumbent fold set that trended N-S and verged to the west. Mineral lineations defining F1 and F2 are recorded by hornblende and plagioclase, indicating both fold sets formed around peak metamorphism. The sharp contrast in hinge direction of F2 (E-W) to F1 (N-S) was likely due to the onset of the Neoacadian orogeny and the oblique collision of the Carolina superterrane to the Laurentian margin during that time.

The channel flow model along with the orogen-parallel translation model lacks shear kinematic capability with what was found in the Cusseta quadrangle. The most likely model is klippe kinematics, which is the model suggested to represent how this area of the Dadeville Complex was deformed and emplaced. The emplacement of the Dadeville Complex and migmatites throughout this area is suggested to occur at the same time as the F1 event from the Acadian orogeny. The lack of greenschist overprinting mineral assemblages suggest that this section of the Dadeville Complex was affected very little during the Alleghanian orogeny and the Stonewall Line shows evidence of being a weak shear zone/suture between the two complexes.

APPENDIX A

Table A.1 Thin section data includes mineral assemblage percentages, grain size, and shear sense data (if applicable) with designated rock unit from samples collected. (OCC=Opelika: Loachapoka Schist (LS), Farmville Metagranite (FMG)); (DCC=Dadeville: Ropes Creek Amphibolite (RCA), Waverly Gneiss (WG), Agricola Schist (AS)). (Normal shear (top down)=N), (Reverse shear (top up)=R).

Sample	**Location #**	**UTM N**	**UTM W**	**Mineral Assemblage %**	**Grain Size (mm)**	**Shear Sense**	**Rock Unit**
OCC-CB-01	1	3629610	666831	--	--	--	FMG
OCC-CB-02	2	3629314	665098	qtz~30 af~50 pf~10 bt~10	1-2 1-2 1-2 1-5	N 150^{o}	FMG
OCC-CB-03	3	3624614	659738	--	--	--	LS
OCC-CB-04	13	3627987	663505	qtz~20 af~10 ms~30 bt~40	≤2 ≤2 3-5 3-5	--	LS
OCC-CB-05	16	3628358	663517	--	--	N 140^{o}	LS
OCC-CB-06	16	3628358	663517	--	--	N 140^{o}	LS
OCC-CB-07	16	3628358	663517	gt~10 sill~15 ms~50 bt~25	1-6 1-4 5-10+ 1-3	N 140^{o}	LS
OCC-CB-08	73	3625255	662428	qtz~10 af~50 pf~20 ms~10 bt~10	1 1 ≤1 ≤2 ≤1	R 010^{o}	FMG
DCC-CB-01	4	3626438	659107	--	--	--	RCA
DCC-CB-02	5	3625984	660711	--	--	--	RCA/LS

Sample	Location #	UTM N	UTM W	Mineral Assemblage %	Grain Size (mm)	Shear Sense	Rock Unit
DCC-CB-03	7	3625340	658207	--	--	--	RCA
DCC-CB-04	9	3626667	659100	qtz~15 pf~25 amph~60	<1 <1 ≤2	--	RCA
DCC-CB-05	11	3626759	659100	--	--	--	RCA
DCC-CB-06	19	3625781	656692	qtz~10 pf~30 amph~40 bt~20	<1 <1 1-3 1-2	R 155^o	WG
DCC-CB-07	19	3625781	656692	--	--	R 155^o	WG
DCC-CB-08	19	3625781	656692	qtz~30 pf~40 af~10 bt~20	≤2 ≤1 ≤1 ≤1	R 155^o	WG
DCC-CB-09	20	3623206	652725	--	--	--	RCA
DCC-CB-10	21	3626326	653189	qtz~10 pf~35 af~5 amph~50	<1 ≤1 <1 ≤3	R 270^o	RCA
DCC-CB-11	23	3626678	653499	qtz~20 pf~20 amph~50 px~10	≤1 ≤1 ≤2 ≤2	R 225^o	RCA
DCC-CB-12	24	3628578	654398	qtz~40 pf~50 amph~10	1-2 ≤2 ≤1	--	RCA
DCC-CB-13	25	3628585	654435	qtz~10 pf~40 af~10 amph~40	≤2 ≤2 ≤2 ≤2.5	R 290^o	RCA
DCC-CB-14	29	3629888	654704	--	--	--	RCA
DCC-CB-15	31	3630650	654410	qtz~20 pf~50 af~15 bt~15	≤2 ≤3 ≤1 <1	R 230^o	RCA
DCC-CB-16	32	3630706	654077	qtz~15 pf~35	≤2.5 ≤2.5	N 080^o	WG

Sample	Location #	UTM N	UTM W	Mineral Assemblage %	Grain Size (mm)	Shear Sense	Rock Unit
				af~30 bt~20	≤1 ≤1		
DCC-CB-17	33	3630352	658048	qtz~20 pf~40 amph~40	≤2.5 ≤2 ≤2.5	R 270^o	RCA
DCC-CB-18	34	3627881	650979	qtz~10 pf~40 amph~50	<1 <1 ≤1	--	RCA
DCC-CB-19	35	3633356	655643	qtz~10 pf~40 amph~50	<1 ≤1 ≤2	--	RCA
DCC-CB-20	36	3634115	654288	qtz~30 pf~50 bt~20	≤2 ≤2 ≤1	R 280^o	WG
DCC-CB-21	38	3632599	654728	qtz~20 pf~50 amph~30	≤1 ≤2 ≤1	N 100^o	RCA
DCC-CB-22	40	3633128	654604	qtz~20 pf~45 amph~35	<1 ≤1 ≤1	--	RCA
DCC-CB-23	41	3635041	652962	qtz~5 pf~50 amph~35 px~10	≤1 ≤2.5 ≤2 ≤2	R 275^o	RCA
DCC-CB-24	42	3634323	652618	qtz~25 pf~40 af~15 bt~20	≤2.5 1-2 1-3 ≤2	N 085^o	WG
DCC-CB-25	44	3633219	653443	pf~50 px~50	≤1 ≤1	--	RCA
DCC-CB-26	46	3631782	653472	qtz~20 pf~40 amph~40	≤5 1-2 1-10+	--	RCA
DCC-CB-27	48	3632217	652643	qtz~20 pf~40 amph~30 grt~10	≤2 ≤3.5 ≤3 1-2.5	R 100^o	RCA
DCC-CB-28	49	3636896	653219	qtz~25 pf~40 bt~25 ep~5 grt~5	≤2 ≤2 ≤1 <1 <1	N 180^o	WG

Sample	Location #	UTM N	UTM W	Mineral Assemblage %	Grain Size (mm)	Shear Sense	Rock Unit
DCC-CB-29	55	3637682	655826	amph~20 px~20 chl~40 ky~10 sill~10	1-2 1 ≤1 1-2 ≤1	R 015°	AS?
DCC-CB-30	56	3638170	657772	qtz~25 pf~40 amph~30 bt~5	≤1 ≤2.5 ≤1 ≤1	N 030°	WG
DCC-CB-31	58	3636122	658309	qtz~25 pf~50 amph~10 bt~15	≤1 ≤4 ≤2 ≤1	N 066°	WG
DCC-CB-32	62	3632478	658086	qtz~20 pf~30 amph~50	≤2 ≤4 ≤2.5	N 135°	RCA
DCC-CB-33	63	3637637	659309	qtz~25 pf~40 amph~25 gt~10	≤2.5 ≤2.5 ≤2 ≤2.5	R 273°	WG
DCC-CB-34	68	3630372	662784	qtz~15 pf~25 amph~60	≤5 ≤1 ≤1	R 235°	RCA
DCC-CB-35	69	3628873	659055	qtz~20 pf~40 af~15 bt~25	≤2 ≤2.5 ≤2.5 ≤3	R 122°	WG
DCC-CB-36	72	3633956	654944	--	--	--	RCA

Table A.2 Field and lab measurements with associated outcrops and their shear sense with designated rock unit. (OCC=Opelika: Loachapoka Schist (LS), Farmville Metagranite (FMG)); (DCC=Dadeville: Ropes Creek Amphibolite (RCA), Waverly Gneiss (WG), Agricola Schist (AS)). (Normal shear (top down)=N), (Reverse shear (top up)=R).

Sample	**Location #**	**UTM N**	**UTM W**	**Min. Foliations (S/D/DD)**	**Lineation (P→T)**	**Shear Sense**	**Rock Unit**
OCC-CB-01	1	3629610	666831	--	--	--	FMG
OCC-CB-02	2	3629314	665098	050 37 NW 210 42 NW 046 44 NW 230 49 NW 224 54 NW 235 42 NW 230 40 NW	47→340	N 150°	FMG
OCC-CB-03	3	3624614	659738	052 40 NW 036 52 NW 279 32 NE 256 34 NW 266 32 NW 255 35 NW	15→008	--	LS
OCC-CB-04	13	3627987	663505	144 47 SW 137 19 SW 143 32 SW 156 24 SW 144 44 SW	11→169 11→160 09→157	--	LS
--	14	3628060	663564	181 40 NW 215 16 NW 170 17 SW	--	--	LS
--	15	3628279	663673	194 20 NW 153 24 SW 175 24 SW 188 42 NW 187 31 NW	--	--	LS
OCC-CB-05	16	3628358	663517	194 28 NW 205 16 NW 195 24 NW 198 21 NW 205 21 NW 220 15 NW	13→319 13→326 13→321	N 140°	LS

Sample	Location #	UTM N	UTM W	Min. Foliations (S/D/DD)			Lineation (P→T)	Shear Sense	Rock Unit
OCC-CB-06	16	3628358	663517	220	12	NW	--	N 140°	LS
OCC-CB-07	16	3628358	663517	021 030 034 044 005	23 28 20 14 25	NW NW NW NW NW	--	N 140°	LS
OCC-CB-08	73	3625255	662428	010 011 225 039 170 190 185	36 36 25 25 36 38 39	SE SE SE SE NE SE SE	03→182	R 010°	FMG
DCC-CB-01	4	3626438	659107	022 033 056 215 164 079 058 206 219 215 189 240	81 79 75 87 13 32 45 84 82 80 44 46	NW NW NW NW SW NW NW NW NW NW NW NW	26→023	--	RCA
DCC-CB-02	5	3625984	660711	062 060 305 014 200 285 185 195 255 135 194	48 35 32 26 57 39 29 56 30 32 26	NW NW SW NW NW SW NW NW NW SW NW	39→195	--	RCA/ LS
--	6	3625192	657449		--		--	--	RCA
DCC-CB-03	7	3625340	658207	194 180 174 212 216 051 253	33 34 28 09 18 05 26	NW W SW NW SE SE SE	--	--	RCA

Sample	Location #	UTM N	UTM W	Min. Foliations (S/D/DD)	Lineation (P→T)	Shear Sense	Rock Unit
				190 35 SE 053 15 SE 074 09 SE 075 08 SE 125 21 SW 165 31 SW 186 27 NW			
--	8	3626598	659103	229 88 NW 236 78 SE 208 76 SE 230 58 NW 225 83 SE 220 39 NW 211 45 NW 045 89 SE 040 86 SE	--	R 155^{o}	RCA
DCC-CB-04	9	3626667	659100	191 25 NW 207 28 NW 020 22 NW 209 32 NW 195 18 NW	16→354	--	RCA
--	10	3626734	659097	261 48 NW 274 39 NE 270 35 N 246 49 NW 245 44 NW	26→059 33→046 37→040	--	RCA
DCC-CB-05	11	3626759	659100	144 38 SW 128 35 SW 130 40 SW 140 49 SW 151 34 SW 146 30 SW	--	--	RCA
--	12	3626842	659097	264 25 SE 265 20 SE 270 22 S 089 19 SE	--	--	RCA
--	17	3630676	665130	217 87 SE 021 82 NW	--	--	RCA
--	18	3626586	656909	234 11 NW 262 16 NW 248 10 NW 260 14 NW	--	--	RCA
DCC-CB-06	19	3625781	656692	149 24 SW 205 11 SE	11→110 11→114	R 155^{o}	WG

Sample	Location #	UTM N	UTM W	Min. Foliations (S/D/DD)	Lineation (P→T)	Shear Sense	Rock Unit
				117 21 NE 145 09 NE 210 16 SE 334 03 SW 113 07 NE 002 20 SE	06→350 06→345		
DCC-CB-07	19	3625781	656692	"	"	R 155°	WG
DCC-CB-08	19	3625781	656692	"	"	N 155°	WG
DCC-CB-09	20	3623206	652725	332 47 NE 327 46 NE 322 43 NE	--	--	RCA
DCC-CB-10	21	3626326	653189	010 54 SE	50→070	R 270°	RCA
--	22	3627202	653650	009 56 NW 012 57 NW	--	--	RCA
DCC-CB-11	23	3626678	653499	016 39 SE 010 54 SE 200 46 SE	--	R 255°	RCA
DCC-CB-12	24	3628578	654398	025 47 SE 054 28 SE 225 40 SE	02→230 03→060	--	RCA
DCC-CB-13	25	3628585	654435	196 64 SE 185 81 SE 024 54 SE	54→103	R 290°	RCA
--	26	3629492	654526	240 32 SE 215 54 SE	--	--	RCA
--	27	3629560	654555	250 76 SE 220 59 SE 240 60 SE	--	--	RCA
--	28	3629663	654608	198 66 SE 199 54 SE 193 69 SE	--	--	RCA
DCC-CB-14	29	3629888	654704	242 58 SE 230 58 SE	--	--	RCA
--	30	3630651	654573	044 67 SE 055 48 SE	--	--	RCA
DCC-CB-15	31	3630650	654410	018 24 SE 163 26 NE 183 12 SE	23→130	R 230°	RCA
DCC-CB-16	32	3630706	654077	183 42 SE 187 42 SE 200 32 SE	42→090	N 080°	WG

Sample	Location #	UTM N	UTM W	Min. Foliations (S/D/DD)	Lineation (P→T)	Shear Sense	Rock Unit
DCC-CB-17	33	3630352	658048	148 54 NE 185 44 NE 162 59 NE	53→071	R 270°	RCA
DCC-CB-18	34	3627881	650979	354 31 NE 344 24 NE 355 31 NE	03→171	--	RCA
DCC-CB-19	35	3633356	655643	356 14 NE 359 27 NE 200 30 SE 009 21 SE 002 21 SE 000 29 E 012 19 SE	02→007	--	RCA
DCC-CB-20	36	3634115	654288	341 26 NE 336 36 NE 321 36 NE 190 39 NE 130 38 NE	17→132	R 280°	WG
--	37	3632345	654866	100 29 NE 116 32 NE 170 33 NE 276 40 NE 187 36 SE 098 46 NE 165 27 NE 130 38 NE 125 36 NE	19→084	--	RCA
DCC-CB-21	38	3632599	654728	030 47 SE 035 53 SE 040 51 SE 055 43 SE	52→108	N 100°	RCA
--	39	3632908	654754	201 41 SE 18 22 SE 121 40 NE 032 59 SE 175 38 NE 180 29 E 200 41 SE	--	--	RCA
DCC-CB-22	40	3633128	654604	014 47 SE 192 50 SE 191 41 SE	32→058 08→187	--	RCA

Sample	Location #	UTM N	UTM W	Min. Foliations (S/D/DD)			Lineation (P→T)	Shear Sense	Rock Unit
DCC-CB-23	41	3635041	652962	202	36	SE	29→087	R 275^o	RCA
				246	38	SE			
				006	48	SE			
				006	29	SE			
				358	42	NE			
DCC-CB-24	42	3634323	652618	259	36	SE	14→085	N 085^o	WG
				254	34	SE			
				258	19	SE			
				234	26	SE			
--	43	3633846	652719	237	64	SE	--	--	RCA
				230	63	SE			
				235	64	SE			
				242	56	SE			
DCC-CB-25	44	3633219	653443	353	72	NE	--	--	RCA
				335	79	NE			
--	45	3633595	652552	214	27	SE	--	--	RCA
				227	29	SE			
				232	31	SE			
DCC-CB-26	46	3631782	653472	054	36	SE	--	--	RCA
				042	30	SE			
				030	29	SE			
				027	21	SE			
				019	28	SE			
--	47	3631909	652940	066	26	SE	--	--	RCA
				068	22	SE			
				225	23	SE			
				245	23	SE			
DCC-CB-27	48	3632217	652643	259	29	SE	04→069	R 100^o	RCA
				244	34	SE			
				257	28	SE			
				270	19	S			
				284	24	SW			
DCC-CB-28	49	3636896	653219	351	20	NE	07→180	N 180^o	WG
				194	25	SE			
				007	26	SE			
				349	32	NE			
--	50	3637086	652752	193	25	SE	--	--	RCA
				195	39	SE			
				236	34	SE			
				220	19	SE			
--	51	3639399	654462	194	20	SE	--	--	RCA
				041	25	SE			
				024	12	SE			
				184	14	SE			

Sample	Location #	UTM N	UTM W	Min. Foliations (S/D/DD)	Lineation (P→T)	Shear Sense	Rock Unit
				206 03 SE 346 43 NE 015 34 SE			
--	52	3637030	653898	236 36 SE 231 26 SE 200 36 SE 247 46 SE 202 20 SE 202 36 SE 232 38 SE	--	--	RCA
--	53	3637434	655470	166 20 NE 167 23 NE 162 23 NE 214 40 SE 200 20 SE	--	--	RCA
--	54	3637034	655777	239 30 SE 265 16 SE	--	--	RCA
DCC-CB-29	55	3637682	655826	205 36 SE 211 37 SE 215 42 SE	15→198	R 015°	AS?
DCC-CB-30	56	3638170	657772	182 29 SE 189 34 SE 192 44 SE 187 30 SE 020 35 SE	27→125 29→062 08→033	N 030°	WG
--	57	3637846	6588497	101 24 NE 110 18 NE 145 12 NE 180 05 E 145 14 NE 105 10 NE	--	--	WG
DCC-CB-31	58	3636122	658309	209 26 SE 210 24 SE 209 32 SE 215 19 SE 216 39 SE 031 27 SE	10→66	N 066°	WG
--	59	3635691	658242	009 28 SE 188 22 SE 201 19 SE 009 25 SE 003 29 SE 187 32 SE	32→088	--	RCA

Sample	Location #	UTM		Min. Foliations (S/D/DD)			Lineation (P→T)	Shear Sense	Rock Unit
		N	W						
--	60	3634800	658255	000	41	E	--	--	RCA
				355	44	NE			
				191	42	SE			
				156	42	NE			
				205	43	SE			
				184	36	SE			
				152	40	NE			
				169	40	NE			
				187	51	SE			
--	61	3633782	658176	060	51	SE	--	--	WG
				226	62	SE			
				237	57	SE			
				225	46	SE			
				226	54	SE			
				226	75	SE			
DCC-CB-32	62	3632478	658086	226	73	SE	67→105	N	RCA
				224	75	SE	69→113	135^{o}	
				214	74	SE	72→135		
				230	71	SE			
				225	72	SE			
DCC-CB-33	63	3637637	659309	206	28	SE	31→087	R	WG
				200	25	SE	23→085	273^{o}	
				219	46	SE			
				216	42	SE			
				190	28	SE			
				203	34	SE			
--	64	3637014	662637	241	44	SE	--	--	RCA
				221	57	SE			
				205	64	SE			
				246	34	SE			
				225	90				
				310	34	NE			
				176	35	NE			
				177	40	NE			
				232	70	SE			
				021	57	SE			
				062	32	SE			
--	65	3633551	663471	075	15	NW	--	--	RCA
				076	29	NW			
				115	54	NE			
				130	38	NE			
--	66	3633985	663114	184	50	SE	--	--	RCA
				164	46	NE			

Sample	Location #	UTM N	UTM W	Min. Foliations (S/D/DD)	Lineation (P→T)	Shear Sense	Rock Unit
--	67	3638386	663301	270 65 S 272 66 SW 254 45 SE 249 43 SE	18→099	--	RCA
DCC-CB-34	68	3630372	662784	068 41 SE 066 33 SE 138 58 SW 170 47 W 126 48 SW 034 69 SE 041 53 SE 054 38 SE 056 22 SE 235 55 SE	21→058	R 235°	RCA
DCC-CB-35	69	3628873	659055	103 08 NE 046 11 SE 110 20 NE	08→313	R 122°	WG
--	70	3631916	658885	134 45 NE 151 53 NE 145 48 NE 191 55 SE 191 49 SE 186 45 SE 201 56 SE	--	--	RCA
--	71	3632123	659661	066 40 SE 061 34 SE 064 61 SE 052 66 SE 256 81 SE 064 76 SE 057 73 SE 045 56 SE 064 36 SE	58→207 65→100	--	RCA
DCC-CB-36	72	3633956	654944	329 75 NE 165 53 NE 161 33 NE 140 25 NE	--	--	RCA

REFERENCES

Allmendinger, R. W., Cardozo, N., and Fisher, D., 2012, Structural geology algorithms: Vectors and tensors in structural geology: Cambridge University Press.

Bentley, R. D., and Neathery, T. L., 1970, Geology of the Brevard fault zone and related rocks of the Inner Piedmont of Alabama, in Bentley, R. D., and Neathery, T. L., eds., Geology of the Brevard fault zone and related rocks of the Inner Piedmont of Alabama: Tuscaloosa, Alabama Geological Society, 8th Annual Field Trip Guidebook, p. 1–79.

Bittner, E.I., and Neilson, M.J., 1990, Structural and metamorphic development of the Dadeville Complex, emphasizing the Dadeville and Agricola shear zones, *in* Steltenpohl, M. G., Neilson, M. J., and Kish, S. A., editors, Geology of the southern Inner Piedmont, Alabama and southwest Georgia, Geological Society of America Southeastern section 39th Annual Meeting Fieldtrip Guidebook: Tuscaloosa, Alabama, Geological Survey of Alabama, p. 91–99.

Cardozo, N., and Allmendinger, R.W., 2013, Spherical projections with OSXStereonet: Computers and Geosciences, v. 51, p. 193–205.

Drummond, M.S., Neilson, M.J., Allison, D.T., and Tull, J.F., 1997, Igneous petrogenesis and tectonic setting of granitic rocks from the eastern Blue Ridge and Inner Piedmont, Alabama Appalachians: Memoir of the Geological Society of America, v. 191, p. 147–164, doi:10.1130/0-8137-1191-6.147.

Farris, D.W., Tull, J., Mueller, P., and Davis, B., 2017, Is the Dadeville Complex part of the “missing” southern Appalachian Taconic arc?, *in* Barineau, C., and Tull, J., editors, A Taconic Backarc and arc terrane in the southern Appalachians:

Correlating geologic units of the Blue Ridge and western Inner Piedmont of Georgia and Alabama: Georgia Geological Society 51st Annual Fieldtrip Guidebook, p. 41–56.

Goldberg S.A., and Steltenpohl M.G., 1990, Timing and Characteristics of Paleozoic Deformation and Metamorphism in the Alabama Inner Piedmont: American Journal of Science, v. 290, p. 1169–1200.

Hatcher, R.D., et. al., 2015, Alleghanian orogen, *in* The Appalachian-Ouachita Orogen in the United States, p. 233–318, doi:10.1130/dnag-gna-f2.233.

Hatcher R.D., Bream B.R., Merschat A.J., 2007, Tectonic map of the southern and central Appalachians: A tale of three orogens and a complete Wilson Cycle, in Hatcher R. D. Jr.., Carlson M. P., McBride J. H., Martínez Catalán J. R., editors, 4-D Framework of Continental Crust: Geological Society of America, Memoirs, v. 200, p. 595–632, doi:https://doi.org/10.1130/2007.1200(29).

Hatcher, R.D., Merschat, A.J., 2006, The Appalachian Inner Piedmont: an exhumed strike-parallel, tectonically forced orogenic channel, *in* Geological Society Special Publication, Geological Society of London, v. 268, p. 517–541, doi:10.1144/GSL.SP.2006.268.01.24.

Huebner, M.T., Hatcher, R.D., and Merschat, A.J., 2017, Confirmation of the southwest continuation of the Cat Square terrane, southern Appalachian Inner Piedmont, with implications for middle Paleozoic collisional orogenesis: American Journal of Science, v. 317, p. 95 LP – 176, doi:10.2475/02.2017.01.

Ma, C., Foster, D.A., Hames, W.E., Mueller, P.A., and Steltenpohl, M.G., 2019, From the Alleghanian to the Atlantic: Extensional collapse of the southernmost Appalachian orogen: Geology, v. 47, p. 367–370, doi:10.1130/G46073.1.

Ma, C., Vandervoort, D.S., Steltenpohl, M.G., and Schwartz, J.J., 2019, Formation and orogen-parallel transport of the Dadeville Complex, Alabama, USA: Implications for the Taconian orogeny in the southern Appalachians: American Journal of Science, v. 319, p. 582–630, doi:10.2475/07.2019.03.

Merschat, A.J., Hatcher, R.D., and Davis, T.L., 2005, The northern Inner Piedmont, southern Appalachians, USA: Kinematics of transpression and SW-directed mid-crustal flow: Journal of Structural Geology, v. 27, p. 1252–1281, doi:10.1016/j.jsg.2004.08.005.

Neilson, M.J., and Stow, S.H., 1986, Geology and geochemistry of the mafic and ultramafic intrusive rocks, Dadeville belt, Alabama.: Geological Society of America Bulletin, v. 97, p. 296–304, doi:10.1130/0016-7606(1986)97<296:GAGOTM>2.0.CO;2.

Osborne, W.E., Szabo, M.W., Neathery, T.L., Copeland, C.W., Jr, 1988. Geologic map of Alabama, Northeast sheet. Geological Survey of Alabama Special Map 220, scale 1:250,000.

Perkins, D., Henke, K.R., 2003, Minerals in Thin Section, p. 175.

Ramsay, J.G., 1967, Folding and fracturing of rocks: New York, McGraw-Hill, p. 568.

Ramsay, J.G., and Huber, M.I., 1987, The techniques of modern structural geology, v. 2: Folds and Fractures: London, Academic Press, p. 392.

Sawyer, E.W., 2008, Working with migmatites: nomenclature for the constituent parts. *In* Working with Migmatites (E.W. Sawyer & M. Brown, eds.). Mineralogical Association of Canada Short Course 38, Quebec City Quebec, p. 1-28.

Sears, J.W., Cook, R.B., and Brown, D.E., 1981, Tectonic evolution of the western part of the Pine Mountain window and adjacent Inner Piedmont Province, in Sears, J.W., ed., Contrasts *in* Tectonic Style between the Inner Piedmont Terrane and the Pine Mountain Window: Tuscaloosa, Alabama, Alabama Geological Society, 18th Annual Field Trip Guidebook, p. 1–13.

Snoke, A.W., and Frost, B.R., 1990, Exhumation of high pressure pelitic schist, Lake Murray spillway, South Carolina; evidence for crustal extension during Alleghanian strike-slip faulting: American Journal of Science, v. 290, p. 853–881, doi:10.2475/ajs.290.8.853.

Snoke, A.W., and Mosher, S., 1989, The Alleghanian Orogeny As Manifested In The Appalachian Internides, *in* p. 288–318.

Solar, G.S., 2008, The interplay between tectonics/structure and migmatite morphology in the field, *In* Working with Migmatites (E.W. Sawyer & M. Brown, eds.). Mineralogical Association of Canada Short Course 38, Quebec City Quebec, p. 145-158.

Steltenpohl, M.G., 1988, Kinematics of the Towaliga, Bartletts Ferry, and Goat Rock fault zones, Alabama: the late Paleozoic dextral shear system in the southernmost Appalachians: Geology, v. 16, p. 852–855, doi:10.1130/0091-7613(1988)016<0852:KOTTBF>2.3.CO;2.

Steltenpohl, M.G., and Kunk, M.J., 1993, 40 Ar/ 39 Ar thermochronology and Alleghanian development of the southernmost Appalachian Piedmont, Alabama and southwest Georgia: Geological Society of America Bulletin, v. 105, p. 819–833, doi:10.1130/0016-7606(1993)105<0819:AATAAD>2.3.CO;2.

Steltenpohl, M.G., Neilson, M.J., Bittner, E.I., Colberg, M.R., & Cook, R.B., 1990, Geology of the alabama inner piedmont terrane. Bulletin - Geological Survey of Alabama, p. 80.

Thiessen, R.L., and Means, W.D., 1980, Classification of fold interference patterns: A reexamination: Journal of Structural Geology, v. 2, p. 311-316.

Tull, J.F., and Holm, C.S., 2005, Structural evolution of a major Appalachian salient-recess junction: Consequences of oblique collisional convergence across a continental margin transform fault: Bulletin of the Geological Society of America, v. 117, p. 482–499, doi:10.1130/B25578.1.

Tull, J.F., Mueller, P.A., Farris, D.W., and Davis, B.L., 2018, Taconic suprasubduction zone magmatism in southern Laurentia: Evidence from the Dadeville Complex: Bulletin of the Geological Society of America, v. 130, p. 1339–1354, doi:10.1130/B31885.1.